Bucceri and Pincus, Esqs.
1200 Route 46
Clifton, New Jersey 07013
(973) 773-5665
Counsel for Plaintiff/Relator, Dr. Helene Z. Hill

UNITED STATES DISTRICT COURT
DISTRICT OF NEW JERSEY

UNITED STATES OF AMERICA EX REL. DR. HELENE Z. HILL,	:	
	:	CASE NO. 03-4837 (DMC)
PLAINTIFF,	:	
v.	:	
UNIVERSITY OF MEDICINE & DENTISTRY: OF NEW JERSEY, DR. ROGER W. HOWELL and DR. ANUPAM BISHAYEE,	:	
DEFENDANTS.		

CERTIFICATION OF DR. HELENE Z. HILL IN OPPOSITION TO MOTION TO QUASH SUBPOENA ISSUED TO DR. THOMAS HEI

Dr. Helene Z. Hill, being of full age and realizing the consequences of the certification appearing below, says:

1. I am the Plaintiff/Relator in the above captioned action and, as such, have personal knowledge of the facts set forth in this certification. I make this certification in opposition to the motion to quash the subpoena that was served on Dr. Thomas Hei, and which required that he appear for a deposition noticed to take place on July 9, 2008. The deposition was temporarily adjourned by consent in order to allow Dr. Hei to file a motion to quash the subpoena. For the reasons which follow, I respectfully request that the motion to quash be denied.

BACKGROUND

2. This is an action to recover damages and civil penalties on behalf of the United States of America arising from false statements and claims made and presented by the defendants and/or their agents, employees and co-conspirators in violation of the Federal Civil False Claims Act, 21 U.S.C. § 3729 et.seq. as amended (the "Act"). The violations of the Act involve the Defendants' application for, and subsequent receipt of, federal grant monies (Grant No. R01CA83838) based upon the knowing submission of a grant application to the United States Department of Health and Human Services, National Institute of Health (NIH). That application (as revised), as well the findings of certain experiments that were subsequently undertaken, were supported with data, statements and records that were false or fraudulent.

3. Defendant Howell's revised grant application set forth a proposal to research the effects of non-uniform distributions of radioactivity and to delineate a biological

mechanism known as the bystander effect. The designated outcome of the research was to achieve a better understanding and prediction of the biological response of tumor and normal tissue to non-uniform distributions of radioactivity.

4. Howell's proposal raised significant issues in diagnostic and therapeutic nuclear medicine. His proposed studies would be of significance to patients, since the risk of radiation insult can be drastically underestimated and potentially lead to increased risk of inducing cancer. In contrast, some patients can be over- or under- treated in radionuclide therapy of cancer. Both scenarios can thus present adverse consequences in the final outcome for the patient. **It is, therefore, critical that patients not be misled about the results of the research.**

5. On two occasions preceding the submission of the revised grant application, I observed Howell's Research and Teaching Specialist, the Defendant, Bishayee, engaged in preliminary experiments. My observations led me to believe that Bishayee was falsifying the data underlying the experiments and the conclusions reached by Howell from those experiments.

6. I informed Howell of my observations and suspicions relating to Bishayee. Notwithstanding this fact, Howell dismissed my concerns and further refused to intercede to my request to investigate Bishayee's actions. Instead, Howell determined to use the results of Bishayee's experiments as part of the preliminary data supporting his revised grant application to NIH.

7. Howell further presented in his grant application data purporting to show a bystander effect using Tritiated Thymidine (Grant application page 26, Figure 2, circles). These and similar data were presented in 2 publications (Bishayee, *et al.* Radiation

Research 152: 88 (1999), Figures 3 circles and 6 inverted triangles; Bishayee, *et al.* Radiation Research 155: 335 (2001) Figure 2A) (Exhibits 1 and 2).

8. In or about March 2001, Dr. Lenarczyk, a post-doctoral fellow employed in Dr. Howell's lab, observed and reported to me that he also suspected Bishayee of fabricating data. Lenarczyk reported that he had observed Bishayee setting up an experiment with contaminated cultures. In light of this fact, I and Lenarczyk documented the management of the experiment by Bishayee.

9. As a result of these actions, both I and Lenarczyk concluded that Bishayee had, in fact, fabricated the experiment's data and engaged in scientific fraud. On or about April 10, 2001, I reported the findings to Howell and to the Radiology Department Chair, Dr.Stephen Baker.

10. The matter was thereafter referred to Defendant, University of Medicine and Dentistry of New Jersey Campus Committee on Research Integrity. In July, 2001 the Committee concluded that there was no cause to warrant further proceedings.

11. During the course of the Committee's review of my complaint, Defendant Howell was ordered to conduct a series of other experiments in order to replicate the data which he had reported in the grant. **These data could not be replicated in 6 trials performed in April – September 2001 and were at extreme variance with a total of 22 experiments performed from October 2000 through September 2001 by Drs. Howell and Lenarczyk.**

THE BASIS FOR THE SUBPOENA TO DR. THOMAS HEI

12. Notwithstanding the inability of Howell to replicate the data as ordered by the Committee, the Defendants have asserted that, because other researchers have been able to replicate the bystander effect using tritiated thymidine, my claim should necessarily fail. In this regard, it is my understanding that the Defendants are referring to a research article entitled (R. Persaud, H. Zhou, S. Baker, T. Hei, and E. Hall),"Assessment of Low Linear Energy Transfer Radiation-Induced Bystander Mutagenesis in a Three-Dimensional Culture Model", Cancer Res 2005; 65 (21) (November 1, 2005)(Exhibit 3). The individuals who performed the experiments and wrote the paper are associated with the Center for Radiological Research, Columbia University Medical Center, New York, New York.

13. However, my review of that research paper suggests that the experiment protocols that were used by Persaud, Zhou, Baker, Hei and Hall, appear to differ in important ways from the experiment protocols utilized by Bishayee and Howell. Howell could not, using experiment protocols that were used by Bishayee, replicate Bishayee's bystander effect using V79 cells which are a line of Chinese hamster cells similar to the cells used by the Columbia group. Nor could he or Lenarczyk, using Bishayee's protocols, replicate the bystander effect using CHO cells, as the Columbia researchers have reported. However certain of Howell's and Lenarczyk's results using uniformly labeled cells are similar to those of the Columbia group in that the survivals are biphasic (i.e. rather than being a simple exponential decline in survival, there is first a rapid decline in survival followed by a change in slope and slower decline in survival). Notwithstanding, Howell presented in his grant application data purporting to show that cells uniformly labeled with tritiated thymidine exhibit an exponential decrease in

survival when exposed to increasing doses of tritiated thymidine (grant application Fig. 2 triangles, 1999 paper Fig 3 triangles and Fig 7 inverted triangles; 2001 paper Fig 1 open circles and squares). These data as presented in the grant application and in the two Bishayee reports are also at variance with those reported by Persaud, et. al. Fig 3 circles.

14. It is, moreover, significant to note that the Columbia paper also cites to the articles written and cited by Howell in his revised grant application (See, Exhibit 3, Page 9876, f.n. 3 and 5). These are the two (2) papers that are identified in Paragraph 7 above (Exhibits 1 and 2).

15. In light of the above, my counsel undertook to subpoena Dr. Hei for a deposition. The purpose of the deposition is to specifically identify and review the protocols that were utilized in the experiments leading to the Columbia paper (Exhibit 3). Doing so will establish the differences noted above and serve to refute any suggestion by the Defendants that, because other researchers have been able to replicate the bystander effect using tritiated thymidine, my claim should necessarily fail.

THE BASIS WHY F.R.CIV.P 45(C)(3)(B)(ii) DOES NOT SERVE TO BAR THE DEPOSITION OF DR. HEI

16. Contrary to the assertion of Dr. Hei, his deposition is not being sought for purposes of having him disclose an unretained expert's opinion or information that does not describe specific occurrences in dispute and/or resulting from a study that was not requested by a party. While I acknowledge having contacted him for assistance in finding individual(s) who might serve as expert witnesses in this case, I am not requesting him to

serve as my expert. I will have my own expert witness(es), and I do not want Dr. Hei to serve as my expert in this case.

In light of the above, Dr. Hei should be clearly seen to have factual knowledge of the protocols used in his experiments of the bystander effect using tritiated thymidine and CHO cells and which were reported in Exhibit 3. His knowledge and identification of those protocols directly relate to the specific occurrences in dispute in this case and which were cited in his article (Exhibits 1 and 2). As noted, these latter articles (Exhibits 1 and 2) are the very articles that had been cited by Howell in support of the grant forming the basis for this suit.

Based on his experiments, Hei should have an intimate knowledge of the procedures and protocols that were followed by the Howell laboratory and may have even tried these procedures and protocols in his or his post-doctoral assistant's initial experiments. His lab had access to the protocols followed by the Howell lab as they are clearly defined in the Howell papers and were published well before the Columbia studies took place.

The Columbia lab paper does not, however, set forth the protocols and procedures in the manner that the Howell lab did. Howell, however, cites them as confirming his results.

But it appears that that the Columbia lab changed their experiment protocols in some important ways, including but not limited to, (a) using different tubes with a larger capacity than the Helena tubes used by Howell; (b) used a different incubation time for the incubation in the cold (72 hours for Howell)(24 hours for Hei/Hall). There had to be a factual basis for why the Columbia lab did not follow the Howell protocols.

17. Questioning Dr. Hei concerning the protocols will then allow myself and/or my expert(s) to compare those protocols to the protocols used by Bishayee and Howell. Any opinions stemming from those comparisons will be based on our analyses that are separately undertaken without Dr. Hei. Under the circumstances, I respectfully reiterate that Dr. Hei is more properly seen as having knowledge of the facts relevant to this case rather than being asked to give an opinion based on those facts.

18. I would also note that the studies reported by the Columbia lab were supported by public monies (Grants: US DOE DE-FG-03R63441 and NIH CA 49062 and ES 11804). Given this fact and the public interest I have cited earlier, I submit that the public has the right to know what procedures were followed during the course of the experiments even though the rationale for final presentation in their report is not explicitly stated. Viewed in this fashion, it is neither appropriate nor correct for Hei to claim that these requests amount to a taking of intellectual property, as the experiments performed in the laboratory are more properly seen as the property of the United States government. As such, this Court should hold that such alleged property be available to its citizens. Hei's deposition testimony will thus provide factual information that is otherwise unavailable regarding the possibility of hypoxia in the tubes used by Howell (Helena or similar tubes) as well as the time course of the development of hypoxia in the tubes used by Hei/Hall. It will also provide factual information that is otherwise unavailable regarding the kinetics of the cell kill of the uniformly (100%) labeled cells.

19. Given the above, I further submit that any opinions Dr. Hei may have about those facts, have previously been formed and reported in the research paper (Exhibit 3).

He is not being asked to form any new opinions. He is simply being asked about the facts underlying previously formed opinions.

20. Dr. Hei should also be seen as being a unique witness and one among the group of authors for which there is little likelihood that a comparable witness can be found to testify. The Columbia lab is the only other one (besides the Howell lab) that has published results of experiments involving the bystander effect using tritiated thymidine. Quashing Hei's subpoena would result in undue hardship because there is no other person outside of that lab in the world who would have the intimate knowledge to answer these questions of fact regarding its experiments.

21. There is another yet another basis for the deposition of Dr. Hei. I had a conversation with Dr. Hei in which he told me that he had reservations about Dr. Howell's studies. I wish to confirm that conversation and question him as to the facts on which he relied to form such reservations.

22. Compliance with the subpoena will not cause oppression or hardship to Dr. Hei. I have agreed not to require Dr. Hei to travel to New Jersey for the deposition. We are more than willing to travel to Columbia University in New York to take the deposition and minimize any inconvenience to Dr. Hei. Moreover, Dr. Hei does not appear to claim financial problems with testifying. He simply alleges that he might have to expend time to review the notebooks of his experiments. Inasmuch as the Court has the discretion under the rules to order that he be compensated for such time, such claim of hardship is diminimus.

23. For all of the foregoing reasons, I respectfully request that the motion to quash the subpoena be denied. Should, however, the Court be inclined to grant the motion, I

again note that I have been made aware of the fact that, in lieu of quashing or modification, the Court may consider ordering compliance under specified conditions, including reasonable compensation to Dr. Hei. I respectfully submit that my certification demonstrates the need for the testimony that cannot otherwise be obtained without undue hardship to my cause. In the event the Court deems it necessary to order that Dr. Hei be reasonably compensated for his time in deposition, I wish the Court to know that, in the alternative, I am willing to do so.

CERTIFICATION

The foregoing statements made by me are true to the best of my knowledge and belief. I am aware that if any of the foregoing statements made by me are willfully false, I am subject to punishment.

Helene Z. Hill

Dr. Helene Z. Hill

Dated: August 1, 2008

RADIATION RESEARCH 152, 88–97 (1999)
0033-7587/99 $5.00

Evidence for Pronounced Bystander Effects Caused by Nonuniform Distributions of Radioactivity using a Novel Three-Dimensional Tissue Culture Model

Anupam Bishayee, Dandamudi V. Rao and Roger W. Howell[1]

Division of Radiation Research, Department of Radiology, New Jersey Medical School, University of Medicine and Dentistry of New Jersey, Newark, New Jersey 07103

Bishayee, A., Rao, D. V. and Howell, R. W. Evidence for Pronounced Bystander Effects Caused by Nonuniform Distributions of Radioactivity using a Novel Three-Dimensional Tissue Culture Model. *Radiat. Res.* 152, 88–97 (1999).

A new *in vitro* multicellular cluster model has been developed to assess the impact of nonuniform distributions of radioactivity on the biological response of mammalian cells, and the relative importance of bystander effects compared to conventional radiation effects. Chinese hamster V79 cells are labeled with tritiated thymidine ([^{3}H]dThd), mixed with unlabeled V79 cells, and centrifuged gently to form multicellular clusters about 1.6 mm in diameter. The short range of the ^{3}H β particles effectively allows only self-irradiation of labeled cells and no cross-irradiation of unlabeled cells. The percentage of labeled cells is controlled precisely by varying the number of labeled cells mixed with unlabeled cells prior to assembling the cluster. The clusters are assembled in the absence or presence of 100 μ*M* lindane, a chemical that is known to inhibit formation of gap junctions. After the clusters are maintained at 10.5°C for 72 h, the cells are dispersed and plated for colony formation. In the case of 100% labeling, the survival of cells in the cluster depends exponentially (SF = $e^{-A/1.8}$) on the cluster activity *A* (in kBq), and lindane has no effect on the response. A two-component exponential response is obtained for 50% labeling in the absence of lindane (SF = 0.33 $e^{-A/0.81}$ + 0.67 $e^{-A/11.8}$), and lindane has a marked effect on the response (SF = 0.33 $e^{-A/1.6}$ + 0.67 $e^{-A/41.6}$). These data suggest that bystander effects play an important role in the biological response of V79 cells when the ^{3}H is localized in the cell nucleus and distributed nonuniformly among the cells. In contrast, bystander effects cannot be detected above traditional radiation effects (i.e. direct + indirect) when the ^{3}H is localized in the cell nucleus and distributed uniformly among the cells. These results indicate that this multicellular cluster model is well suited for studying the effects of nonuniform distributions of radioactivity, including bystander and "hot-particle" effects. Furthermore, these results suggest that bystander effects may play an important role in the prediction of the biological effects of radiopharmaceuticals used in medical diagnosis and treatment. © 1999 by Radiation Research Society

INTRODUCTION

Over the past several years there have been several reports that cells that have received no radiation exposure suffer biological consequences when they are in the presence of cells that have been irradiated (*1–5*). This phenomenon has been termed the bystander effect. Nagasawa and Little (*1*) used acute external beams of α particles to irradiate monolayers of Chinese hamster ovary cells with low doses. These exposures led to the formation of sister chromatid exchanges in 30–50% of the cells despite the fact that statistically only about 1% of the cell nuclei could have been traversed by an α particle. They concluded that genetic damage can be imparted to "bystander" cells when cell populations are exposed to low doses from α particles. Similar observations were made by Deshpande *et al.* (*2*). Azzam *et al.* (*5*) studied the mechanisms of the bystander effect by showing that the expression levels of TP53, CDKN1A, CDC2, CCNB1 and RAD51 are significantly modulated when human diploid cell populations are irradiated with low doses of α particles where only a small fraction of the nuclei are actually hit. They also found that the extent of modulation was significantly reduced when lindane, an inhibitor of gap-junction intercellular communication (*6, 7*), was present during the irradiation period. These data suggest that gap-junction intercellular communication may play an important role in the bystander effect.

While the studies described above involve the use of α particles, Mothersill and Seymour (*4*) have irradiated cells with γ rays to study the bystander effect. In this case, the gap-junction inhibitor phorbol myristate acid actually increased killing by the bystander effect. Based on these data, they suggested that signal transduction mechanisms, as op-

[1] Author to whom correspondence and requests for reprints should be addressed.

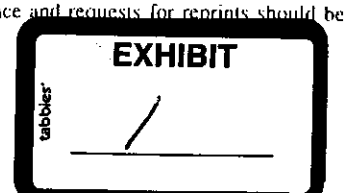

posed to the release of a factor that is directly cytotoxic, may control death or survival due to the bystander effect.

The studies of Nagasawa and Little (*1*), Deshpande *et al.* (*2*) and Mothersill and Seymour (*4*) raise interesting points regarding the biological effects of ionizing radiation, in particular the bystander effect. As noted by these authors and others (*3, 8, 9*), the bystander effect is particularly relevant to the "hot-particle" problem as well as the biological effects of incorporated radionuclides in general. However, there remain several aspects to be addressed such as: (1) What is the significance of the bystander effect compared to the overall effect to the cell when it experiences damage from both bystander and traditional radiation effects (i.e. direct + indirect)? (2) Can bystander effects be observed in three-dimensional tissue models? (3) Do bystander effects indeed result from nonuniform distributions of radioactivity? (4) If so, what types of ionizing radiation produce significant bystander effects? The present work attempts to address some of these questions using a novel three-dimensional cell culture model and precisely controlled nonuniform distributions of incorporated radionuclides to deliver radiation exposures.

MATERIALS AND METHODS

Radiochemical and Quantification of Radioactivity

Tritiated thymidine [^{3}H]dThd) was obtained from NEN Life Science Products (Boston, MA) as a sterile aqueous solution at a concentration of 37 MBq/ml and a specific activity of 3000 GBq/mmol. The activity of ^{3}H was measured with a Beckman LS3800 automatic liquid scintillation counter (Fullerton, CA) by transferring aliquots of radioactive culture medium into 6 ml of Aquasol™ liquid scintillation cocktail (NEN Research Products, Boston, MA). The detection efficiency for the 5.7 keV β particles emitted by ^{3}H was 0.65. The radionuclide ^{3}H has a physical half-life of 12.3 years and emits β particles with a mean energy of 5.67 keV (*10*) corresponding to a mean range in water of about 1 μm (*11*).

Cell Line

Chinese hamster V79 lung fibroblasts (kindly provided by A. I. Kassis, Harvard Medical School, Boston, MA) were used in the present study, with clonogenic survival serving as the biological end point. V79 cells are known to exhibit some degree of gap-junction intercellular communication at 37°C (*12, 13*). The cells were cultured in minimum essential medium (MEM) supplemented with 10% heat-inactivated (57°C, 30 min) fetal calf serum with 2 m*M* L-glutamine, 50 U/ml penicillin and 50 μg/ml streptomycin (MEMA). The pH of the culture medium was adjusted to 7.0 with $NaHCO_3$. All media and supplements used in this study were from Life Technologies (Grand Island, NY). Cells were maintained in 175-cm^2 Falcon sterile tissue culture flasks (Becton Dickinson, Lincoln Park, NJ) at 37°C and 5% CO_2, 95% air, and were subcultured twice weekly or as required.

Radiolabeling and Assembly of Multicellular Clusters with 50% of Cells Labeled

V79 cells growing as monolayers in 175-cm^2 Falcon flasks were washed with 10 ml of phosphate-buffered saline, trypsinized with 0.05% trypsin–0.53 m*M* EDTA, and suspended at 2 × 10^6 cells/ml in calcium-free MEM with 10% heat-inactivated (57°C, 30 min) fetal calf serum, 2 m*M* L-glutamine, 50 U/ml penicillin and 50 μg/ml streptomycin (MEMB). Aliquots of 1 ml were placed in two sets of sterile 17 × 100-mm Falcon polypropylene round-bottom culture tubes (10 tubes in each set) and placed on a rocker-roller (Fisher Scientific, Springfield, NJ) for 3–4 h at 37°C in an atmosphere of 95% air and 5% CO_2. After this conditioning period, 1 ml of MEMB containing various activity concentrations (0–296 MBq) of [^{3}H]dThd was added to the first set of culture tubes containing 1 ml of V79 cells. Only 1 ml of MEMB was added to the other set of tubes. All tubes were then returned to the rocker-roller at 37°C, 95% air and 5% CO_2. After a 12-h period of labeling with radioactivity, the first set of tubes were removed and centrifuged at 2000 rpm at 4°C for 10 min. Aliquots of the supernatant were used to check the concentrations of radioactivity added. The cells were washed three times with 10 ml of MEM with 10% heat-inactivated (57°C, 30 min) calf serum, 2 m*M* L-glutamine, 50 U/ml penicillin and 50 μg/ml streptomycin (wash MEMA). The cells in the second set of tubes (unlabeled) were similarly washed and the contents of a given tube transferred to one of the first set of tubes containing radiolabeled cells. Finally, the pooled cells in each tube were suspended in 400 μl of MEMA or 0.58% DMSO (Sigma Chemical Co., St. Louis, MO) in MEMA or 0.58% DMSO–100 μ*M* lindane (hexachlorocyclohexane, γ-isomer from Sigma) and transferred directly to a sterile 400-μl polypropylene microcentrifuge tube with attached cap (Helena Plastics, San Rafael, CA) (Fig. 1). The concentration of lindane (i.e. 100 μ*M*) was selected based on a separate study as described below, and DMSO served as a control for lindane. The 400-μl tubes were centrifuged at 1000 rpm for 5 min at 4°C to form a multicellular cluster ~1.6 mm in diameter. The resulting cluster contained a total of 4 × 10^6 cells, of which 50% were labeled (Fig. 1). The capped

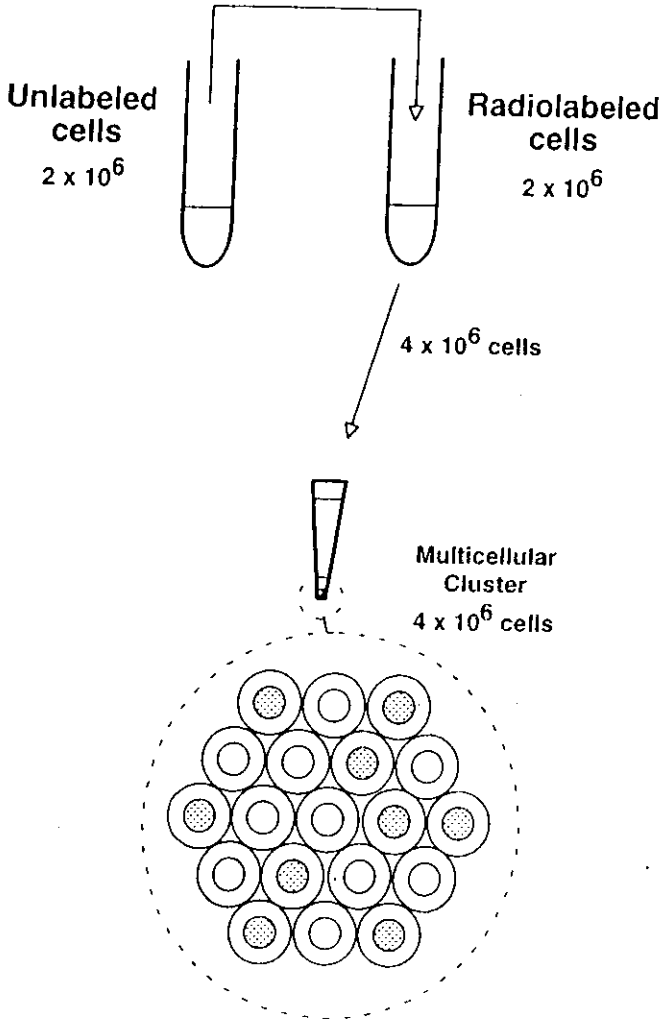

FIG. 1. Assembly of multicellular cluster of V79 cells in which 50% of the cells are radiolabeled with [^{3}H]dThd.

microcentrifuge tubes containing the clusters were placed in a perforated microcentrifuge tube rack and transferred to a refrigerator at 10.5°C. This temperature was selected because V79 cells can remain in the cluster configuration at this temperature for long periods (up to 72 h) without a decrease in plating efficiency. This was also true for V79 cells in suspension culture (*14*). Therefore, the cells accumulate the preponderance of their radioactive decays while in the cluster configuration as opposed to the radiolabeling and colony-forming periods. After 72 h at 10.5°C, the supernatant was carefully removed and the tube was vortexed to disperse the cell cluster. The cells were resuspended in MEMA, transferred to 17 × 100-mm Falcon polypropylene tubes, washed three times with 10 ml of wash MEMA, resuspended in 2 ml of MEMA, passed through a 21-gauge needle five times to disperse cells, and serially diluted (four 10× dilutions), and 1 ml of the appropriate dilutions (approximately 200 cells for control tubes) was seeded in triplicate into 60 × 15-mm Falcon tissue culture dishes. The dishes were then placed in an incubator at 37°C with 95% air and 5% CO_2. Aliquots were taken from each tube before serial dilution, and the mean radioactivity per cell was determined (*15*). The tissue culture dishes were removed from the incubator after 1 week, and the resulting colonies were washed 3 times with normal saline and 2 times with methanol and finally stained with 0.05% crystal violet. The colonies were counted under fluorescent light. A colony count of 25–250 was considered as a valid data point for each tissue culture dish. The surviving fraction compared to the parallel control was determined for each radioactivity concentration employed.

Chemotoxicity and Optimum Concentration of Lindane

Multicellular clusters were prepared wherein 50% of the cells were labeled with a fixed activity concentration of [^{3}H]dThd (148 MBq/ml) as described above. The clusters were maintained at 10.5°C for 72 h in the presence of 20–200 μ*M* of lindane. To achieve this, lindane was first dissolved in DMSO (5 mg/ml), filtered through a Millex®-HV filter (Millipore Corporation, Bedford, MA), and subsequently diluted with MEMA to a final concentration 20–200 μ*M* lindane, 0.58% DMSO. Parallel controls were established where clusters of unlabeled cells were maintained at the same concentrations of lindane with 0.58% DMSO. Thus, for each concentration of lindane, two tubes were prepared—one having a cluster of radiolabeled cells (50%) and one having a cluster of unlabeled cells. After 72 h the cluster was dismantled, the mean activity per cell was determined, and the cell survival was compared to that of its matched control using the procedure outlined above.

Assembly of Multicellular Clusters with 100% Radiolabeled Cells

Multicellular clusters in which 100% of the cells were radiolabeled were assembled using the cells prepared as above. In short, 1 ml of MEMB containing different concentrations of radioactivity was added to culture tubes containing 1 ml of conditioned cells (4 × 10^6 cells). Half of the concentrations used for the 50% labeling experiment were used to maintain approximately the same cluster activity. After an incubation period of 12 h at 37°C in an atmosphere of 95% air and 5% CO_2, the radiolabeled cells (4 × 10^6) were washed as above, suspended in 400 μl of MEMA, 0.58% DMSO in MEMA, or 0.58% DMSO–100 μ*M* lindane in MEMA, and transferred to a 400-μl microcentrifuge tube and centrifuged as described above. The microcentrifuge tubes containing the cell clusters were maintained at 10.5°C for 72 h, after which the surviving fraction of cells was determined as described above.

Response of Multicellular Clusters to Chronic and Acute Exposure to External γ Rays

Microcentrifuge tubes containing multicellular clusters prepared with 4 × 10^6 unlabeled cells as described above were transferred to a refrigerator at 10.5°C. The tubes were placed at different distances from a 370-MBq ^{137}Cs source housed in a small stainless steel capsule. Two control tubes were similarly maintained at 10.5°C without radiation exposure. The cumulated absorbed dose to the irradiated cells was measured using a Thomson-Nielson (Ottawa, Canada) miniature MOSFET dosimeter system. After 72 h of chronic irradiation, the cells were processed as described above to determine the surviving fraction. Cumulated doses of 2.4 to 12.7 Gy were delivered over 72 h at dose rates from 3 to 18 cGy/h, depending on the distance from the source. The response of the multicellular cluster to acute ^{137}Cs γ rays was also studied by maintaining identically prepared multicellular clusters at 10.5°C for 72 h and then irradiating them acutely at the same temperature in a J. L. Shepherd Mark I irradiator (San Fernando, CA). The acute dose rate was ~1–1.7 Gy per minute and total doses ranged from 1 to 12.5 Gy. After the acute irradiation, the cells were processed as above and the surviving fraction was determined compared to that for unirradiated control cells.

Gap-Junctional Intercellular Communication at 10.5°C

The scrape-loading and dye transfer technique of El-Fouly *et al.* (*12*) was used with slight modification. Approximately 4 × 10^6 cells were thawed from a stock of V79 cells maintained at −70°C, washed with MEMA, and immediately plated in a 30-mm Corning tissue culture dish (Corning, NY) with 2 ml of fresh MEMA. The dish was placed in an incubator at 37°C, 95% air and 5% CO_2 for 1 h and was then transferred to a refrigerator at 10.5°C. After 72 h, the confluent cell population was rinsed three times with Ca^{2+}-Mg^{2+}-free PBS. Two milliliters of PBS containing 0.05% Lucifer yellow (Molecular Probes, Inc., Eugene, OR) was added to the dish at room temperature and the monolayer was scraped along three parallel lines using a sterile scalpel blade. The dish was placed in the dark for 5 min to complete dye transfer. As Lucifer yellow is a hydrophilic fluorescent dye with a low molecular weight (mol. wt. 457.2), it can traverse gap junctions and therefore is an efficient means by which to monitor gap-junctional intercellular communication. The dye solution was decanted, the dish was rinsed three times with fresh PBS, and 2 ml of PBS was added to the dish. The plate was observed with an Olympus BX60 epifluorescence phase-contrast microscope illuminated with an Osram HBO 200 W lamp.

RESULTS

Response of Multicellular Clusters to External γ Rays

Figure 2 shows the dose–response curves for multicellular clusters of V79 cells exposed to chronic (3–18 cGy/h) and acute (1–1.7 Gy/min) ^{137}Cs γ irradiation. A least-squares fit of these data to the linear-quadratic model [$SF = \exp(-\alpha D - \beta D^2)$] yielded α(chronic) = 0.0440 ± 0.0183 Gy^{-1}, β(chronic) = 0.00391 ± 0.00231 Gy^{-2}, α(acute) = 0.118 ± 0.025 Gy^{-1}, and β(acute) = 0.00566 ± 0.0042 Gy^{-2}.

Response of Multicellular Clusters to [^{3}H]dThd

Figure 3 shows the surviving fraction of cells in the multicellular cluster as a function of the ^{3}H activity in the cluster when either 50% or 100% of the cells are radiolabeled. The response curve for 100% labeling is exponential, whereas the curve for 50% labeling is two-component exponential. A least-squares fit of these data to a two-component exponential function yields

$$SF = (1 - b)\, e^{-A/A_1} + b\, e^{-A/A_2}, \qquad (1)$$

where SF is the surviving fraction, A is the cluster activity, and b, A_1, and A_2 are the fitted parameters. For 50% labeling, the fitted parameters b, A_1, and A_2 are 0.67 ± 0.12, 0.81 ± 0.56 kBq, and 11.8 ± 3.1 kBq, respectively. In the

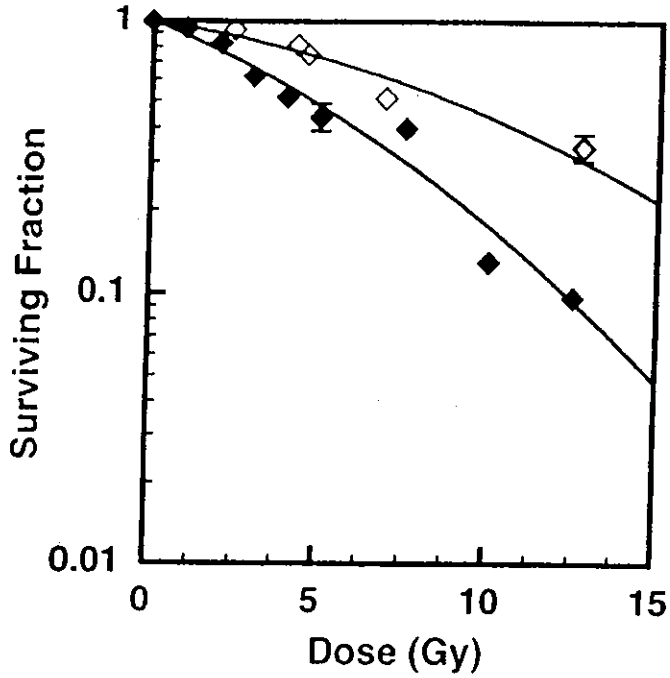

FIG. 2. Survival of V79 cells after acute (♦) and chronic (◊) irradiation of multicellular clusters with ^{137}Cs γ rays. Irradiations were carried out at 10.5°C. The acute dose rate was ~1–1.7 Gy per minute. For chronic irradiation, the tubes containing clusters were placed at different distances from a 370-MBq ^{137}Cs source housed in a small stainless steel capsule. After the acute and chronic irradiation, the clusters were dismantled, cells were processed, and the surviving fraction was determined compared to cells from unirradiated control clusters. Representative standard deviations are indicated by the error bars. Solid curves represent least-squares fits to the linear-quadratic model.

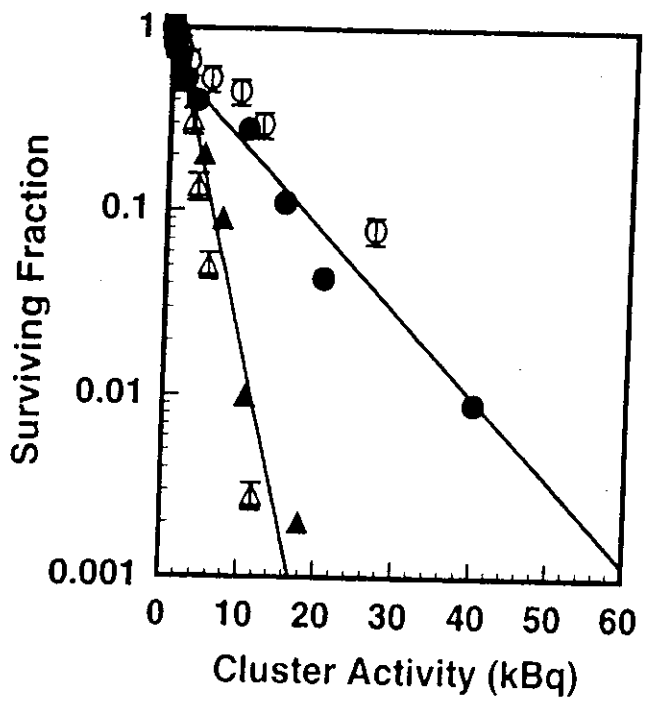

FIG. 3. Survival of V79 cells as a function of cluster activity of [^{3}H]dThd. Data are shown for experiments where 50% (●, ○) or 100% (▲, △) of the cells were radiolabeled in multicellular clusters which were maintained at 10.5°C for 72 h and then the surviving fraction was determined compared to unlabeled cells. Data from two independent experiments are plotted for each labeling condition and are differentiated by open and closed symbols. Representative standard deviations are indicated by the error bars.

case of 100% labeling, with $b = 0$, the fitted value of A_1 is 2.44 ± 0.11 kBq.

Chemotoxicity of Lindane

Figure 4 shows the fraction of surviving cells in multicellular clusters of V79 cells after a 72-h exposure to different concentrations of lindane in the culture medium. The surviving fraction compared to that for untreated controls remains close to unity up to about 100 μ*M* lindane, whereupon a significant decrease is observed. These data suggest that concentrations in excess of 100 μ*M* are not desirable for experiments involving inhibition of gap-junction intercellular communication due to associated cytotoxicity.

Optimum Concentration of Lindane to Inhibit Bystander Effect

Determination of the optimum concentration of lindane to minimize bystander effects is an essential element of the present study. Figure 5 shows the surviving fraction of V79 cells in multicellular clusters as a function of lindane concentration in the cell culture medium. In these experiments, 50% of the cells in the cluster are radiolabeled with approximately 4.8 mBq/cell of [^{3}H]dThd for a total cluster

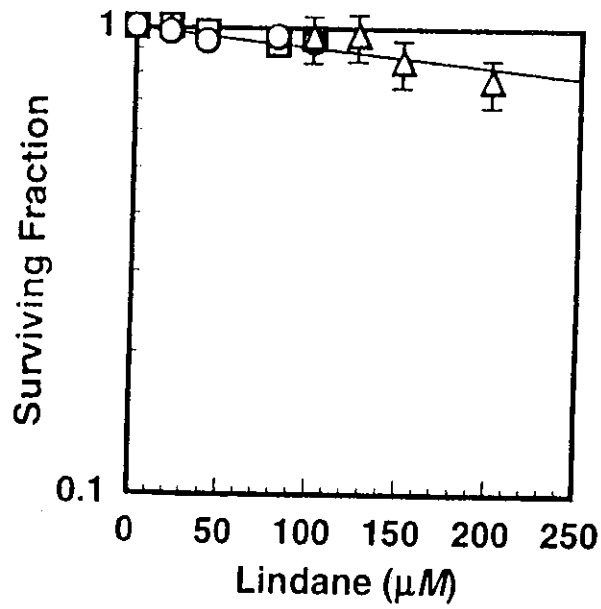

FIG. 4. Chemotoxicity of lindane when V79 multicellular clusters were exposed to the chemical at 10.5°C for 72 h. Representative standard deviations for individual data points are shown. Data from three independent experiments are indicated by different symbols (○, □, △).

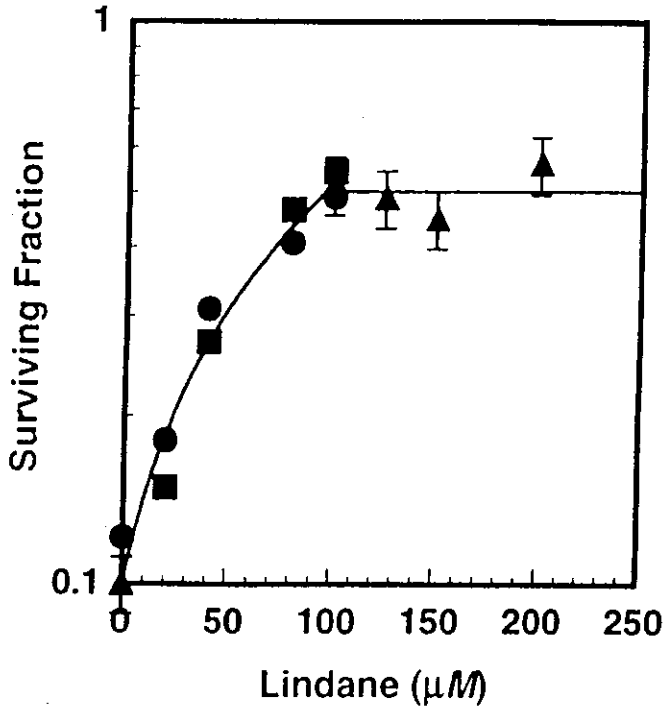

FIG. 5. Effect of lindane concentration on survival of V79 cells from multicellular clusters in which 50% of the cells are labeled with [^{3}H]dThd. The surviving fraction increased steadily with increasing lindane concentration up to 100 μM, after which no additional protective effect was observed. Data from three independent experiments are indicated by three symbols (●, ■, ▲). Representative standard deviations are indicated by the error bars.

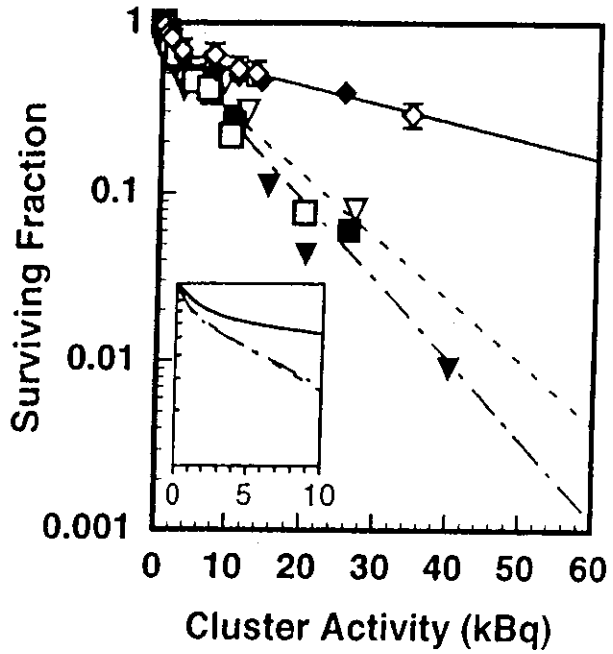

FIG. 6. Survival of V79 cells as a function of cluster activity of [^{3}H]dThd when 50% of the cells were labeled. Multicellular clusters were maintained at 10.5°C for 72 h in the presence of (1) [^{3}H]dThd (▼, ▽; data reproduced from Fig. 3); (2) [^{3}H]dThd + 0.58% DMSO (■, □); or (3) [^{3}H]dThd + 0.58% DMSO + 100 μM lindane (◆, ◇). Data from two independent experiments are plotted for each treatment condition and are differentiated as open and closed symbols. Representative standard deviations are indicated by the error bars. The short-dashed, long-short dashed, and solid curves represent least-squares fits of the data to Eq. (1) for cases 1, 2 and 3, respectively.

activity of about 19 kBq. Multicellular clusters treated with neither [^{3}H]dThd nor lindane served as controls. The concentration of lindane in the culture medium has a marked impact on the surviving fraction of cells in the cluster, elevating the fraction from about 10% at 0 μM lindane to about 50% at 100 μM lindane for multicellular clusters with 50% labeled cells. No further significant increase in surviving fraction was observed at lindane concentrations in excess of 100 μM. These data indicate that 100 μM is the optimum concentration of lindane for carrying out detailed studies of bystander effects in V79 cell multicellular clusters.

Response of Multicellular Clusters to [^{3}H]dThd in the Absence and Presence of Lindane

Figure 6 shows the surviving fraction of cells in the multicellular cluster as a function of the ^{3}H activity in the cluster when only 50% of the cells are radiolabeled. In the absence of lindane, when the cluster activity increases, the surviving fraction decreases sharply to about 50% and then continues to decrease albeit with a more shallow slope. Essentially the same curve is obtained when these clusters are maintained in the presence of 0.58% DMSO. In contrast, clusters that were maintained in the presence of 0.58% DMSO + 100 μM lindane show a similar sharp decrease in the slope of the response curve to about 50% survival and only limited cell killing at higher cluster activities. A least-squares fit of these data to Eq. (1) in the case of 100 μM lindane gives values of 0.67 ± 0.03, 1.6 ± 0.3 and 41.6 ± 5.8 kBq for b, A_1 and A_2, respectively. The fitted parameters for the three irradiation conditions are summarized in Table 1.

The surviving fraction of cells in multicellular clusters assembled with 100% of the cells radiolabeled with [^{3}H]dThd is shown in Fig. 7 as a function of the cluster activity for the three experimental conditions: (1) [^{3}H]dThd, (2) [^{3}H]dThd + 0.58% DMSO, and (3) [^{3}H]dThd + 0.58% DMSO + 100 μM lindane. The fraction of cells surviving compared to untreated controls was calculated in each case. The survival curves in all three cases are single-component exponential, which is commensurate with our earlier studies that examined the radiotoxicity of [^{3}H]dThd in V79 cells maintained in suspension culture (*14*). Least-squares fits of these data to Eq. (1) with $b = 0$ give A_1 values of 2.7 ± 0.1, 2.7 ± 0.2, and 2.8 ± 0.1 kBq for cases 1, 2 and 3, respectively. The fitted parameters for the three irradiation conditions are summarized in Table 1.

Evidence of Gap-Junctional Intercellular Communication at 10.5°C

To verify the capacity of V79 cells to form intercellular communication through gap junctions during maintenance

TABLE 1
Fitted Parameters for Survival Curves for Multicellular Clusters[a]

Treatment	Percentage cells labeled	b	A_1 (kBq)	A_2 (kBq)
[^{3}H]dFThd[b]	100	0	2.7 ± 0.1	...
[^{3}H]dFThd + 0.58% DMSO[b]	100	0	2.7 ± 0.2	...
[^{3}H]dFThd + 0.58% DMSO + 100 μM lindane[b]	100	0	2.8 ± 0.1	...
[^{3}H]dFThd[c]	50	0.67 ± 0.12	0.81 ± 0.56	11.8 ± 3.1
[^{3}H]dFThd + 0.58% DMSO[c]	50	0.75 ± 0.04	0.70 ± 0.17	9.3 ± 0.7
[^{3}H]dFThd + 0.58% DMSO + 100 μM lindane[c]	50	0.67 ± 0.03	1.6 ± 0.3	41.6 ± 5.8

[a] Standard errors are indicated.
[b] Least-squares fit to data in Fig. 7.
[c] Least-squares fit to data in Fig. 6.

at 10.5°C for 72 h, the transfer of Lucifer yellow dye between neighboring cells was studied in cells in monolayers. As shown in Fig. 8, Lucifer yellow was transferred into contiguous cells after the parallel lines were scraped in the monolayer with a scalpel. The highest intensity of Lucifer yellow was noticed in cells at the periphery of the scraped areas, and a gradient of decreasing intensity is evident as the dye spreads further into contiguous cells through gap junctions.

DISCUSSION

Radiopharmaceuticals are used widely in clinical medicine to diagnose and treat a variety of medical conditions. It is well known that when radiopharmaceuticals are administered to the patient, the radioactivity localizes in different tissues in the body and its distribution at the macroscopic and microscopic levels is nonuniform. The degree of nonuniformity can vary widely depending on a variety of factors. The biological consequences of nonuniform distributions of radioactivity in a given tissue can also vary substantially. Despite these well-known facts, current internationally accepted methods for assessing risks from diagnostic nuclear medicine procedures assume that the radioactivity is distributed uniformly in organs and tissues and that the biological response depends principally on absorbed dose, radiation type and tissue radiosensitivity (*16*). Bystander effects and other potential consequences of nonuniform distributions of radioactivity are ignored in these risk estimates. The same assumption is frequently made in assessing risks from environmental (e.g. ^{222}Rn) and accidental (e.g. ^{137}Cs, ^{131}I) exposures to radioactivity. Adelstein *et al.* (*17*) and Makrigiorgos *et al.* (*18*) have raised important concerns regarding the assumption of uniform distribution of radioactivity and their impact on risk estimates. However, one of the major stumbling blocks to predicting the biological response of tissues with nonuniform distributions of radioactivity has been the absence of experimental models that allow tight control over the distribution of the radioactivity.

Multicellular Model

The data in the present work have been obtained with a new three-dimensional tissue culture model that has been designed specifically to quantify the impact of nonuniform distributions of radioactivity in tissues on the biological effect of the incorporated radionuclides. It is demonstrated that multicellular clusters can be assembled by mixing suspensions of radiolabeled and nonradiolabeled cells to achieve a controlled degree of nonuniformity of radioactivity in an *in vitro* multicellular cluster model (Fig. 1). This

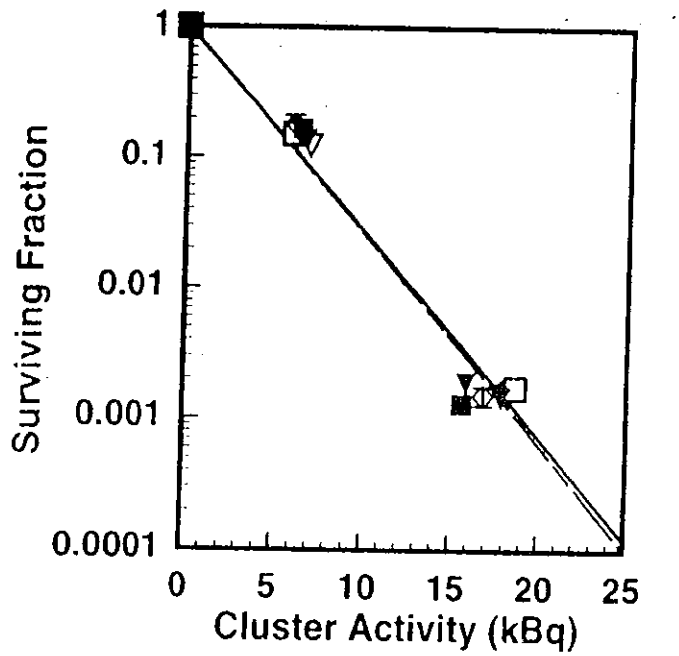

FIG. 7. Survival of V79 cells as a function of cluster activity of [^{3}H]dFThd when 100% of the cells were labeled. Multicellular clusters were maintained at 10.5°C for 72 h in the presence of (1) [^{3}H]dFThd (▼, ▽); (2) [^{3}H]dFThd + 0.58% DMSO (■, □); (3) [^{3}H]dFThd + 0.58% DMSO + 100 μM lindane (♦, ◇). Data from two independent experiments are plotted for each treatment condition and are distinguished as open and closed symbols. Representative standard deviations are indicated by the error bars. The short-dashed, long-dashed and solid curves represent least-squares fits of the data to Eq. (1) for cases 1, 2 and 3 respectively.

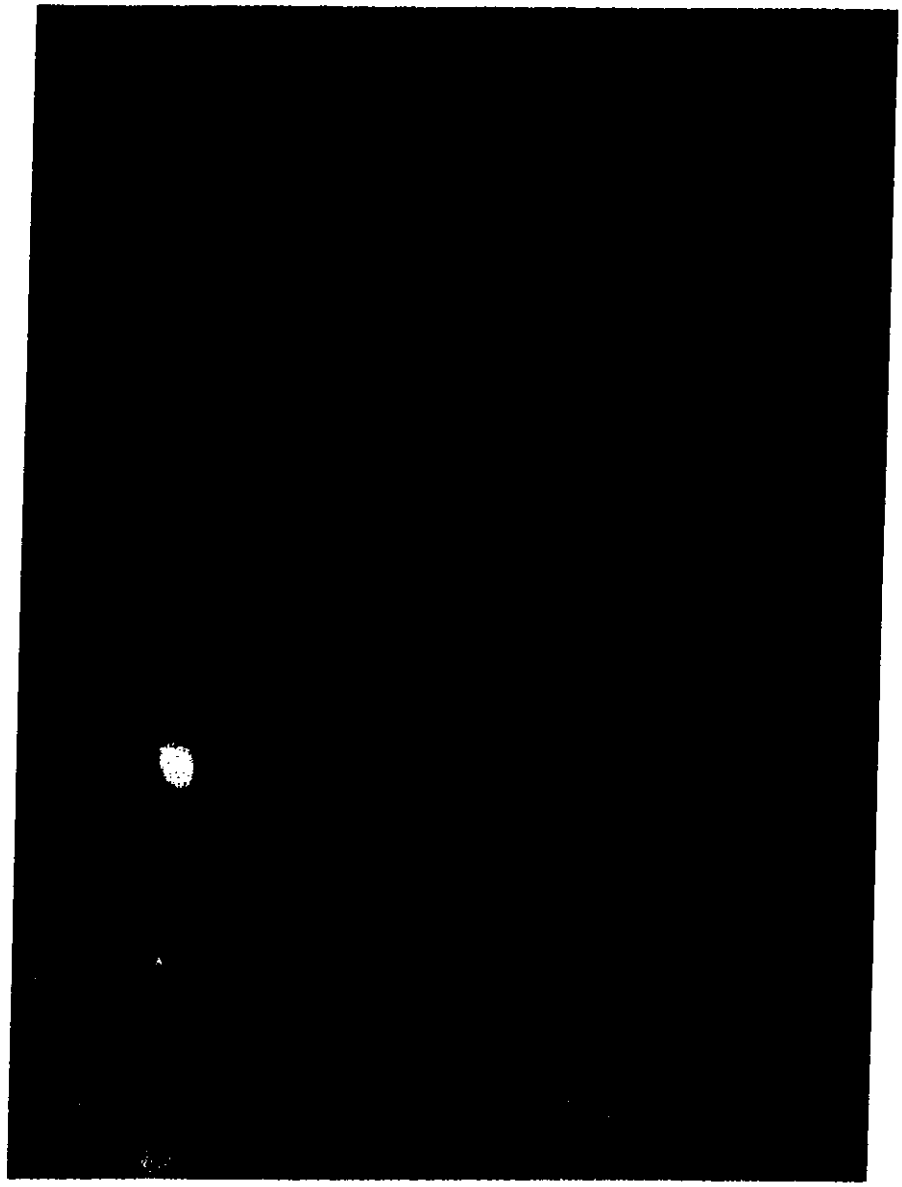

FIG. 8. Transfer of the fluorescent dye Lucifer yellow through gap junctions in V79 cells maintained as a monolayer culture at 10.5 C for 72 h.

new model affords a high degree of control over the percentage of radiolabeled cells in the cluster. The use of different radiochemicals can provide further control over the subcellular distribution of the radioactivity in the labeled cells. These degrees of control over the model are a major departure from past *in vitro* multicellular cluster models wherein multicellular spheroids are prepared prior to treatment with radioactivity, thus leading to a condition where only cells at the periphery of the cluster are effectively labeled (*19, 20*).

The response of the multicellular clusters used in the present work to external beams of ^{137}Cs γ rays is characterized in Fig. 2 for both acute and chronic irradiation. The dose-response curves with shoulders are characteristic of the response of mammalian cells to radiations of low linear energy transfer (LET). The acute doses were delivered at dose rates of 1–1.7 Gy/min, whereas the chronic irradiation was carried out at a dose rate of 3–18 cGy/h. The latter dose rates are more in keeping with those encountered in therapeutic nuclear medicine. Clearly, dose rate has a significant impact on the response.

The survival curves in Fig. 3 correspond to the case where V79 cells are labeled with [^{125}I]dFUdd. The dose responses for 50% and 100% labeling are markedly different from those observed when the cells are irradiated with external γ rays. In the case of 100% labeling of the cells in the cluster, the dose-response curve is exponential with a value of A_1 of 2.44 kBq. This exponential response is commensurate with the response of suspension cultured V79 cells labeled with [^{125}I]dFUdd (*14*). In contrast, the dose-response curve for 50% labeling is two-component exponential, with the second component having a relatively

shallow slope compared to the first component as characterized by the parameters A_1 = 0.81 kBq and A_2 = 11.8 kBq. In other words, for a given amount of ^{3}H radioactivity in the cluster, the two labeling conditions (50%, 100%) yield very different surviving fractions. Therefore, the distribution of radioactivity in the cluster plays an important role in the biological response of the cells in the cluster. This is an important aspect of this new model that can be exploited to obtain quantitative data on the response of multicellular systems to nonuniform distributions of radioactivity.

Another significant feature of this new model is that typical cell survival experiments *in vitro* using radioprotectors or gap-junction inhibitors involve acute radiation exposures in the presence of chemotoxic concentrations of these agents. The cells are usually washed free of the agent immediately after the irradiation and plated for colony formation. When cells are irradiated by incorporated radionuclides, the radiation dose is delivered chronically. To examine the capacity of radioprotectors or gap-junction inhibitors to modify effects caused by chronic irradiation by incorporated radionuclides, the chemical agent should be present throughout the irradiation period (*21*). However, chronic exposure of cultured cells to these chemical agents at 37°C leads to extreme chemotoxicity, particularly when levels sufficient to afford protection are used (*21*). The results in Figs. 4 and 5 show that this problem can be overcome by maintaining the cells at 10.5°C. Under these conditions, the V79 cells did not divide and only minimal chemotoxicity was observed for both control and treated cells when the lindane concentration was maintained at or below 100 μM.

Chinese hamster V79 cells maintained at 37°C have been shown to exhibit intercellular communication through gap junctions. This has been demonstrated by freeze-fracture coupled with quantitative morphology (*13*) as well as the scrape-loading and dye transfer technique (*12*). However, to the best of our knowledge, the capacity of V79 cells to form gap junctions at 10.5°C has not been demonstrated. In the present study, this aspect has been explored by maintaining confluent monolayers of V79 cells at 10.5°C for 72 h and then studying the transfer of the fluorescent dye Lucifer yellow to detect gap-junctional intercellular communication. Figure 8 shows that V79 cells indeed retain their ability to form membrane channels through gap junctions even at 10.5°C, a process that can be seen efficiently through positive dye transfer into contiguous cells.

In view of the versatility and reproducibility of this new multicellular cluster model, it is possible that it may merit consideration for assessing bystander effects as set forth by Mill *et al.* (*8*) in their recent Letter to the Editor. Mill *et al.* (*8*) have argued that to clearly establish the existence of a bystander effect in the case of hot particles (and nonuniform activity distributions in general), "an internationally validated *in vitro* assay together with an internationally validated dosimetry protocol" is needed. The present experimental *in vitro* model, coupled with our theoretical multicellular dosimetry model (*22*), may be considered as a candidate for this purpose. It should be noted, however, that the current experimental protocol uses a maintenance temperature of 10.5°C, which may have an impact on metabolic processes such as DNA repair and cell proliferation. Ward *et al.*, (*23*) have shown that irradiated V79 cells are capable of repairing DNA single-strand breaks at temperatures as low as 10°C, albeit at a reduced rate. Double-strand breaks were not repaired at this temperature. However, despite the dependence of repair on temperature, a 3-h incubation of the irradiated cells at this temperature had no impact on cell survival. Nevertheless, the maintenance temperature in the present model can be increased to 37°C; this will reduce the capacity to introduce adequate concentrations of chemical modifiers such as DMSO and lindane without leading to undesired chemotoxicity.

The Bystander Effect

The β particles emitted by ^{3}H have a spectrum of energies from 0–18.6 keV (*10*) with corresponding ranges in water from 0–7 μm (*24*). The mean energy is only 5.7 keV, which corresponds to a range of only 1 μm in water (*24*). The mean diameter of a V79 cell is 10 μm and its nucleus has a mean diameter of 8 μm (*21*). Since the ^{3}H is incorporated into the DNA of the nuclei of labeled cells, the nuclei in these cells will be efficiently self-irradiated by the low-energy β particles emitted by the radionuclide. However, β particles emitted by ^{3}H decays in the cell nucleus must travel 2 μm (range of 10 keV electron, ref. *24*) just to get from the perimeter of the nucleus of a labeled cell to the perimeter of a nucleus of an unlabeled cell. The distance to the nucleus of the unlabeled cell is considered important because the nucleus presumably contains the primary radiosensitive targets. Since the electrons are emitted by decays occurring randomly throughout the nucleus, nearly all of the β particles will have to travel substantially more than 2 μm just to reach the nucleus of an unlabeled cell. Given that very few of the β particles emitted are in excess of the minimum requirement of 10 keV, the cross-dose received by cells in the cluster is negligible. This premise is supported by the multicellular dosimetry calculations of Goddu *et al.* (*22*) that show that cross-dose for electrons in this energy range is negligible when the radioactivity is localized in the cell nucleus. Therefore, in the absence of bystander effects, one anticipates essentially no killing of unlabeled cells, which should translate into a 50% surviving fraction in the case of 50% labeling at high cluster activities. The steep first component (A_1 = 0.81 kBq) of the two-component dose–response curve in Fig. 3 shows that about 50% of the cells are indeed killed. However, the second component (A_2 = 11.8 kBq) indicates that the unlabeled cells continue to be killed as the activity in the labeled cells is increased even though the unlabeled cells are not significantly irradiated. This suggests that a bystand-

er effect is responsible for the killing of unlabeled cells and, unlike the results of Mothersill and Seymour (*4*), the effect does not saturate with increasing dose (i.e. activity in the labeled cells).

To elucidate the potential mechanisms responsible for the bystander effect observed in Fig. 3, the gap-junction inhibitor lindane was added to the culture medium prior to formation of the multicellular clusters in which 50% of the cells were labeled. Figure 6 shows that 100 μM lindane has a marked impact on the survival of V79 cells with the value of A_2 in Eq. (1) changing from 11.8 kBq to 41.6 kBq. The solvent 0.58% DMSO had no impact on the response of the V79 cells. If the bystander effect blocking factor (BBF) is defined as the ratio

$$\text{BBF} = \frac{A_2 \text{ (with lindane)}}{A_2 \text{ (without lindane)}}, \qquad (2)$$

then the bystander effect blocking factor for 50% labeling of cells in the multicellular cluster with [^{3}H]dThd and maintenance in culture medium with 0.58% DMSO + 100 μM lindane is 3.5 ± 1.0. Since lindane is known to be a gap-junction inhibitor (*6, 7*), and it has been demonstrated in the present study that V79 cells form gap junctions at 10.5°C, it is likely that the bystander effects observed when 50% of the cells in the cluster are labeled with [^{3}H]dThd are due primarily to intercellular communication processes that depend on the formation of gap junctions which connect adjacent cells (*25*).

While lindane is known to be an inhibitor of gap-junction intercellular communication, it is also known to affect other processes that may pertain to its apparent ability to decrease bystander effects. For example, lindane may increase levels of superoxide dismutase and the extent of lipid peroxidation (*26, 27*) and cause alterations in intracellular free calcium and mitochondrial transmembrane potential (*28*). It may also increase the activity of NADPH-cytochrome P450 and the ratio of superoxide anion production/superoxide dismutase activity (*29*) and the formation of reactive oxygen species that result from the metabolism of lindane (*30*). Therefore, it is possible that mitigation of bystander effects by lindane may be due not only to inhibition of gap-junctional intercellular communication but also to these other processes.

Bystander Effects Relative to Conventional Radiation Effects

To assess the relative importance of bystander effects compared to conventional radiation effects (i.e. direct + indirect), the clusters were assembled such that 100% of the cells were again labeled with [^{3}H]dThd. Figure 7 shows the response of multicellular clusters treated with [^{3}H]dThd, [^{3}H]dThd + 0.58% DMSO, or [^{3}H]dThd + 0.58% DMSO + 100 μM lindane. The response of the V79 cells to the three treatment regimens is essentially the same within experimental uncertainties. Each of the cells in the cluster is surrounded by approximately 13 neighbors (*22*). Hence the biological effect imparted to a given target cell in the cluster is due not only to the ^{3}H decays that occur in the target cell but also to the sum of the bystander effects imparted by the neighboring cells. Therefore, since lindane had no impact on cell survival, the contribution of the bystander effect appears to be negligible for this biological end point in the case of 100% labeling, at least over the range of activities considered.

It thus stands to reason that the impact of the bystander effect on cell survival depends on the percentage of cells in the cluster that are labeled, with the effect being most pronounced at low labeling percentages and when cross-irradiation between cells is absent or minimal. Accordingly, it is anticipated that a somewhat smaller bystander effect may be observed when cells are labeled with radionuclides that emit particles with ranges of several cell diameters or more (e.g. ^{125}I) because cross-irradiation plays a more important role in these cases (*22*).

Finally, it should be noted that the arguments made above are based on cell survival data alone. While it is not expected that data based on other biological end points will point toward very different conclusions than those reached above, the importance of examining other end points is recognized.

ACKNOWLEDGMENTS

The authors would like to thank Prof. James E. Trosko, Michigan State University College of Human Medicine, for providing advice and his protocols for the scrape-loading and dye transfer technique. They are also grateful to Dr. Satam Banga, UMDNJ-New Jersey Medical School, for his assistance with the fluorescence microscopy techniques used in this work.

Received: March 31, 1999; accepted: May 6, 1999

REFERENCES

1. H. Nagasawa and J. B. Little, Induction of sister chromatid exchanges by extremely low doses of alpha-particles. *Cancer Res.* 52, 6394–6396 (1992).
2. A. Deshpande, E. H. Goodwin, S. M. Bailey, B. L. Marrone and B. E. Lehnert, Alpha-particle-induced sister chromatid exchange in normal human lung fibroblasts—Evidence for an extranuclear target. *Radiat. Res.* 145, 260–267 (1996).
3. M. Sigg, N. E. A. Crompton and W. Burkhart, Enhanced neoplastic transformation in an inhomogeneous radiation field: An effect of the presence of heavily damaged cells. *Radiat. Res.* 148, 543–547 (1997).
4. C. Mothersill and C. B. Seymour, Cell–cell contact during γ irradiation is not required to induce a bystander effect in normal kidney keratinocytes: Evidence for release during irradiation of a signal controlling survival into the medium. *Radiat. Res.* 149, 252–262 (1998).
5. E. I. Azzam, S. M. de Toledo, T. Gooding and J. B. Little, Intercellular communication is involved in the bystander regulation of gene expression in human cells exposed to very low fluences of alpha particles. *Radiat. Res.* 150, 497–504 (1998).
6. X. Guan and R. J. Ruch, Gap junction endocytosis and lysosomal degradation of connexin43-P2 in WB-F344 rat liver epithelial cells treated with DDT and lindane. *Carcinogenesis* 17, 1791–1798 (1996).
7. K. A. Criswell and R. Loch-Caruso, Lindane-induced elimination of

gap junctional communication in rat uterine monocytes is mediated by an arachidonic acid-sensitive cAMP-independent mechanism. *Toxicol. Appl. Pharmacol.* **135**, 127–138 (1995).

8. A. J. Mill, M. W. Charles and P. J. Darley, Enhanced neoplastic transformation in an inhomogeneous radiation field: An effect of the presence of heavily damaged cells. *Radiat. Res.* **149**, 649–651 (1998). [Letter to the Editor]
9. N. E. A. Crompton, M. Sigg and W. Burkart, Enhanced neoplastic transformation in an inhomogeneous radiation field: An effect of exposure to supralethally damaged cells. *Radiat. Res.* **149**, 651–653 (1998). [Letter to the Editor]
10. E. Browne and R. B. Firestone, *Table of Radioactive Isotopes*. Wiley, New York, 1986.
11. ICRU, *Photon, Electron, Proton and Neutron Interaction Data for Body Tissues*. Report 46, International Commission on Radiation Units and Measurements, Bethesda, MD, 1992.
12. M. H. El-Fouly, J. E. Trosko and C. C. Chang, Scrape-loading and dye transfer: A rapid and simple technique to study gap junctional intercellular communication. *Exp. Cell. Res.* **168**, 422–430 (1987).
13. S. B. Yancey, J. E. Edens, J. E. Trosko, C. C. Chang and J. P. Revel, Decreased incidence of gap junctions between Chinese hamster V-79 cells upon exposure to the tumor promoter 12-*o*-tetradecanoyl phorbol-13-acetate. *Exp. Cell Res.* **139**, 329–340 (1982).
14. R. W. Howell, S. M. Goddu, A. Bishayee and D. V. Rao, Radioprotection against lethal damage caused by chronic irradiation with radionuclides *in vitro*. *Radiat. Res.* **150**, 391–399 (1998).
15. A. I. Kassis and S. J. Adelstein, A rapid and reproducible method for the separation of cells from radioactive media. *J. Nucl. Med.* **21**, 88–90 (1980).
16. ICRP, *Radiation Dose to Patients from Radiopharmaceuticals*. Publication 53. International Commission on Radiological Protection, Pergamon Press, Oxford, 1987.
17. S. J. Adelstein, A. I. Kassis and K. S. R. Sastry, Cellular vs. organ approaches to dose estimates. In *Proceedings of Fourth International Radiopharmaceutical Dosimetry Symposium* (A. T. Schlafke-Stelson and E. E. Watson, Eds.), pp. 13–25. National Technical Information Service, Springfield, VA, 1986.
18. G. M. Makrigiorgos, S. J. Adelstein and A. I. Kassis, Cellular radiation dosimetry and its implications for estimation of radiation risks. Illustrative results with technetium-99m-labeled microspheres and macroaggregates. *J. Am. Med. Assoc.* **264**, 592–595 (1990).
19. V. K. Langmuir, J. K. McGann, F. Buchegger and R. M. Sutherland, The effect of antigen concentration, antibody valency and size, and tumor architecture on antibody binding in multicell spheroids. *Nucl. Med. Biol.* **18**, 753–764 (1991).
20. R. Sutherland, F. Buchegger, M. Schreyer, A. Vacca and J. P. Mach, Penetration and binding of radiolabeled anti-carcinoembryonic antigen monoclonal antibodies and their antigen binding fragments in human colon multicellular tumor spheroids. *Cancer Res.* **47**, 1627–1633 (1987).
21. R. W. Howell, D. V. Rao, D-Y. Hou, V. R. Narra and K. S. R. Sastry, The question of relative biological effectiveness and quality factor for Auger emitters incorporated into proliferating mammalian cells. *Radiat. Res.* **128**, 282–292 (1991).
22. S. M. Goddu, D. V. Rao and R. W. Howell, Multicellular dosimetry for micrometastases: Dependence of self-dose versus cross-dose to cell nuclei on type and energy of radiation and subcellular distribution of radionuclides. *J. Nucl. Med.* **35**, 521–530 (1994).
23. J. F. Ward, C. L. Limoli, P. M. Calabro-Jones and J. Aguilera, An examination of the repair saturation hypothesis for describing shouldered survival curves. *Radiat. Res.* **127**, 90–96 (1991).
24. ICRU, *Stopping Powers for Electrons and Positrons*. Report 37, International Commission on Radiation Units and Measurements, Bethesda, MD, 1984.
25. R. Bruzzone, T. W. White and D. A. Goodenough, The cellular internet: On-line with connexins. *Bioessays* **18**, 709–718 (1996).
26. B. C. Koner, B. D. Banerjee and A. Ray, Organochlorine pesticide-induced oxidative stress and immune suppression in rats. *Ind. J. Exp. Biol.* **36**, 395–398 (1998).
27. B. Descampiaux, J. M. Leroux, C. Peucelle and F. Erb, Assay of free-radical toxicity and antioxidant effect on the Hep 3B cell line: A test survey using lindane. *Cell Biol. Toxicol.* **12**, 19–28 (1996).
28. R. Rosa, E. Rodriguez-Farre and C. Sanfeliu, Cytotoxicity of hexachlorocyclohexane isomers and cyclodienes in primary cultures of cerebellar granule cells. *J. Pharmacol. Exp. Ther.* **278**, 163–169 (1996).
29. K. A. Simon Giavarotti, L. Rodrigues, T. Rodrigues, V. B. Junqueira and L. A. Videla, Liver microsomal parameters related to oxidative stress and antioxidant systems in hyperthyroid rats subjected to acute lindane treatment. *Free Radic. Res.* **29**, 35–42 (1998).
30. P. Perocco, A. Colacci, C. Del Ciello and S. Grilli, Cytotoxic and cell transforming effects of the insecticide, lindane (γ-hexachlorocyclohexane) on BALB/c 3T3 cells. *Res. Commun. Mol. Pathol. Pharmacol.* **89**, 329–339 (1995).

RADIATION RESEARCH 155, 335–344 (2001)
0033-7587/01 $5.00

Free Radical-Initiated and Gap Junction-Mediated Bystander Effect due to Nonuniform Distribution of Incorporated Radioactivity in a Three-Dimensional Tissue Culture Model

Anupam Bishayee,[a] Helene Z. Hill,[a] Dana Stein,[b] Dandamudi V. Rao[a,1] and Roger W. Howell[a,2]

[a] Division of Radiation Research, Department of Radiology, and [b] Department of Pediatrics, University of Medicine and Dentistry of New Jersey-New Jersey Medical School, Newark, New Jersey 07103

Bishayee, A., Hill, H. Z., Stein, D., Rao, D. V. and Howell, R. W. Free Radical-Initiated and Gap Junction-Mediated Bystander Effect due to Nonuniform Distribution of Incorporated Radioactivity in a Three-Dimensional Tissue Culture Model. *Radiat. Res.* 155, 335–344 (2001).

To investigate the biological effects of nonuniform distribution of radioactivity in mammalian cells, we have developed a novel three-dimensional tissue culture model. Chinese hamster V79 cells were labeled with tritiated thymidine and mixed with unlabeled cells; and multicellular clusters (~1.6 mm in diameter) were formed by gentle centrifugation. The short-range β particles emitted by ^{3}H impart only self-irradiation of labeled cells without significant cross-irradiation of unlabeled bystander cells. The clusters were assembled in the absence or presence of 10% dimethyl sulfoxide (DMSO) and/or 100 μ*M* lindane. DMSO is a hydroxyl radical scavenger, whereas lindane is an inhibitor of gap junctional intercellular communication. The clusters were maintained at 10.5°C for 72 h to allow ^{3}H decays to accumulate and then dismantled, and the cells were plated for colony formation. When 100% of the cells were labeled, the surviving fraction was exponentially dependent on the mean level of radioactivity per labeled cell. A two-component exponential response was observed when either 50 or 10% of the cells were labeled. Though both DMSO and lindane significantly protected the unlabeled or bystander cells when 50 or 10% of the cells were labeled, the effect of lindane was greater than that of DMSO. In both cases, the combined treatment (DMSO + lindane) elicited maximum protection of the bystander cells. These results suggest that the bystander effects caused by nonuniform distributions of radioactivity are affected by the fraction of cells that are labeled. Furthermore, at least a part of these bystander effects are initiated by free radicals and are likely to be mediated by gap junctional intercellular communication.

INTRODUCTION

There is substantial interest in the role of bystander effects in the biological response of mammalian cells to ionizing radiation. It has long been believed that the principal genetic effects of ionizing radiation in mammalian cells are the direct result of DNA damage in irradiated cells that has not been repaired adequately. Therefore, when cells are exposed to external beams of radiation, only those cells that receive "hits" from the emitted radiations would be damaged. No effects would be observed in cells that are not "hit." These cells are referred to as bystanders. Studies from a number of laboratories suggest that these bystander cells do indeed incur damage as a consequence of being in the neighborhood of irradiated cells (*1*). Nagasawa and Little (2) first showed that Chinese hamster ovary (CHO) cells exposed to very low fluences of α particles exhibited a much higher incidence of cells with sister chromatid exchanges (SCEs) than expected based on the number of cells that were traversed by α particles. These authors found similar results when induction of *HPRT* mutations was used as the end point, thereby confirming that genetic damage does occur in bystander cells that are not irradiated (*3*). Deshpande *et al.* (*4*) reported increases of more than eightfold in the percentage of primary human fibroblast cells expressing an increased level of SCE over the actual number of nuclei traversed by an α particle. Hickman *et al.* (*5*) documented that α particles induced accumulation of the Tp53 tumor suppressor protein in rat lung epithelial cells in a higher percentage of cells than expected based on the number that would have received a direct nuclear traversal. Azzam *et al.* (*6*) made similar observations with altered expression of TP53, CDKN1A (also known as $p21^{Waf1}$), CDC2 (also known as $p34^{cdc2}$), cyclin B1 and RAD51 in human diploid fibroblast cells. Prise *et al.* (*7*) reported a higher frequency of apoptotic and micronucleated human fibroblast cells in cultures irradiated with a charged $^3He^{2+}$ particle microbeam. Mothersill and Seymour (*8*) demonstrated that addition of medium from epithelial cells irradiated with γ rays led to increased cell death and apoptosis of unirradiated cells.

[1] Present address: 2637 S. Saks Pt., Inverness, FL 34450.
[2] Author to whom correspondence should be addressed at Division of Radiation Research, Department of Radiology, MSB F-451, University of Medicine and Dentistry of New Jersey-New Jersey Medical School, 185 South Orange Avenue, Newark, NJ 07103.

EXHIBIT 2

Although consistent support for the existence of bystander effects is available in the literature, studies that probe the mechanisms that lead to damage in bystander cells are limited. Bystander effects have been attributed to the production of extracellular factors that lead to the generation of reactive oxygen species (ROS) (*9–11*). More recently, Iyer and Lehnert (*12*) have postulated that transforming growth factor β1 is the mediator of α-particle-induced bystander responses. Gap junctional intercellular communication (GJIC) has also been implicated as one of the mechanisms (*6, 13*). It has also been suggested that other mechanisms such as extranuclear-originating signal pathways, secreted diffusible factors, and apoptosis-inducing factors may be involved in the responses of bystander cells (*14, 15*). These findings suggest that different mechanisms may be operational for bystander effects depending on the cell type, the type of radiation, and other experimental conditions, including the end points studied.

The issue of bystander effects is relevant to the biological effects of nonuniform distribution of radioactivity; however, there is a paucity of data. This is of major importance to risk estimation in diagnostic nuclear medicine and radiation protection (e.g. inhalation of radon/radon progeny) as well as clinical outcome in therapeutic nuclear medicine. One of the major obstacles to predicting the biological response of tissues with nonuniform distribution of radioactivity is the absence of suitable experimental models that allow precise control of the degree of nonuniformity. To overcome this problem, we have recently developed a novel three-dimensional tissue culture model (*13*). Using this model, we have shown evidence of pronounced bystander effects in the form of decreased cell survival when ^3H is localized in the DNA of Chinese hamster lung fibroblast (V79) cells and is distributed nonuniformly in multicellular clusters (*13*). In the present communication, the same multicellular cluster model is used to investigate the impact of different magnitudes of nonuniform distribution of radioactivity on bystander effects. The underlying mechanisms of bystander effects that arise from nonuniform distribution of radioactivity are also studied.

MATERIALS AND METHODS

Radiochemical and its Quantification

Tritiated thymidine ([^3H]dThd) was obtained from NEN Life Science Products (Boston, MA) as a sterile aqueous solution at a concentration of 37 MBq/ml with a specific activity of 3000 GBq/mmol. The activity of ^3H was measured with a Beckman LS3800 automatic liquid scintillation counter (Fullerton, CA). The detection efficiency for the β particles emitted by ^3H was 0.65.

Cell Culture

V79 cells, kindly provided by Dr. A. I. Kassis (Harvard Medical School, Boston, MA), were used in the present study, with clonogenic survival serving as the biological end point. V79 cells are known to exhibit some degree of GJIC (*16–18*). The different minimum essential media (MEMA, MEMB and wash MEMA) and culturing conditions have been described in detail previously (*13*). The plating efficiency was about 64%.

Assembly of Multicellular Clusters

The protocols were as described earlier (*13*). Briefly, V79 cells were conditioned in 1 ml MEMB in 17 × 100-mm Falcon polypropylene culture tubes placed on a rocker-roller for 3–4 h in an incubator at 37°C, 5% CO_2, 95% air (2 or 4 × 10^6 cells/ml). Thereafter, 1 ml MEM containing various activities of [^3H]dThd was added and the tubes were returned to the rocker-roller. After 12 h, the cells were washed three times with wash MEMA, resuspended in 2 ml of MEMA, and passed several times through a 21 gauge needle. Additional tubes containing cells not labeled with ^3H were processed identically. The radiolabeled cells were then mixed with unlabeled cells to get 100, 50 or 10% radiolabeled cells, pelleted and transferred directly to a sterile 400-μl polypropylene microcentrifuge tube (Helena Plastics, San Rafael, CA). The tubes were centrifuged at 1000 rpm for 5 min at 4°C to form clusters with diameter ~1.6 mm (4 × 10^6 cells).

Treatment with DMSO and/or Lindane

To study the mechanisms underlying bystander effects, the multicellular clusters were assembled in the presence of the free radical scavenger DMSO and/or an inhibitor of GJIC, lindane (Sigma Chemical Co., St. Louis, MO). To achieve radioprotection, a DMSO concentration of 10% (1.28 *M*) was required as per our previous studies (*19*). Lindane was dissolved in DMSO (5 mg/ml) and subsequently diluted with MEMA to a final concentration of 100 μ*M* lindane–0.58% DMSO. These concentrations of lindane and DMSO were not cytotoxic (*13*).

Cell Survival

The microcentrifuge tubes containing the clusters were maintained at 10.5°C for 72 h to allow decay of ^3H in the absence of cell division. Under these conditions, V79 cells can withstand prolonged exposure to 10% DMSO and 100 μ*M* lindane without significant loss of plating efficiency (*13, 19*). The supernatant was then carefully removed and the tubes were vortexed to disperse the cell clusters. The cells were washed three times with 10 ml of wash MEMA, resuspended in 2 ml of wash MEMA, passed several times through a 21-gauge needle (resulting in a single cell suspension with a doublet frequency of only 2.4%), serially diluted, seeded in triplicate into 60 × 15-mm Falcon tissue culture dishes, and incubated at 37°C with 95% air and 5% CO_2. Aliquots were taken from each tube before serial dilution as above, and the mean radioactivity per cell was determined. After 7 days, the surviving fraction compared to control cells was determined.

Kinetics of Radioactivity in Cells

To ascertain the absorbed dose received by the cells, the kinetics of uptake and clearance of the radioactivity from the cells was followed. Multicellular clusters were prepared with 100% of the cells labeled as described above. At various times after the clusters were placed at 10.5°C, a cluster was dismantled and the level of radioactivity per cell was determined. Additionally, cells from clusters that had been maintained at 10.5°C for 72 h were washed with wash MEMA, and 1 × 10^6, 5 × 10^5, 2.5 × 10^5 and 2.5 × 10^5 cells were finally plated in duplicate into 75-cm^2 culture flasks. On each of the following 4 days, duplicate flasks with the same number of cells plated (in descending order) were removed from the incubator and the activity per cell was determined.

Monitoring of Radioactivity in Labeled and Unlabeled Cells

Studies were carried out to trace radioactivity in the labeled and unlabeled cells. The radiolabeled cells were dyed with 0.05 μ*M* carboxyfluorescein diacetate succinimidyl ester (CFDA SE) in phosphate-buffered saline (PBS) at 37°C for 15 min using a Vybrant® cell tracer kit

(Molecular Probes, Eugene, OR). CFDA SE passively diffuses into cells, where its acetate groups are cleaved by intercellular esterases to yield the highly fluorescent carboxyfluorescein succinimidyl ester that reacts with intracellular amines forming well-retained fluorescent conjugates. The radiolabeled and dyed cells (2×10^6) were mixed with an equal number of unlabeled, undyed cells. The pooled cells were used to form clusters containing a total of 4×10^6 cells (50% of the cells were radiolabeled and dyed) and the clusters were maintained at 10.5°C. After 72 h, the cells from two clusters were pooled, washed with PBS, resuspended in 5 μM EDTA in PBS to a concentration of 10^7 cells/ml, and passed through a 21-gauge needle five times to produce a single cell suspension. The cells were subjected to fluorescence-activated cell sorting (FACS) using a FACSCalibur flow cytometer (Becton Dickinson, San Francisco, CA). An air-cooled 488-nm argon-ion laser was used to excite the dye. The excitation and emission peaks of the fluorescent dye are 492 and 517 nm, respectively. Fluorescence in the FL-1 channel was collected along with forward-angle and 90° light scatter. The cells were sorted for dye-negative cells. A gate was applied around the cell population to evaluate cellular events. Single-parameter histograms based on 10,000 events were analyzed using CellQUEST software (Becton Dickinson). After sorting, the dye-negative cells (unlabeled and undyed) were collected, pooled, washed and finally resuspended in 2 ml of 5 μM EDTA in PBS. Aliquots were used to determine the mean activity per cell. An additional 0.5 ml of the suspension was subjected to FACS for the second time to check the purity of sorted cells (i.e. absence of dye-positive cells).

Assessment of GJIC by Flow Cytometry

The presence of functional GJIC between V79 cells in multicellular clusters maintained at 10.5°C in the absence and presence of lindane was monitored by flow cytometry. The method of Goldberg *et al.* (*20*) was used with modifications. Cells (4 or 2×10^6) were loaded with calcein AM (Molecular Probes). This fluorescent dye becomes membrane impermeant when it enters the cell. However, it can traverse functional gap junctions (*21*). The loading was achieved by incubating cells for 25 min at 37°C in the presence of 2 ml of 20 μM dye in PBS. The cells were then washed with PBS, resuspended in prewarmed MEMA, incubated at 37°C for 30 min, and centrifuged, and the supernatant was decanted. Undyed cells were treated similarly. These cells were used to form multicellular clusters containing 100 or 50% dyed cells. The clusters with 50% dyed cells were prepared in the presence or absence of 100 μM lindane. The clusters were then maintained at 10.5°C for 72 h. The cells from clusters were washed with PBS and resuspended in 1 ml of 5 μM EDTA in PBS. In the lindane-treated cells, all steps after the dyeing procedure, including washes and resuspensions, were carried out in the presence of lindane. GJIC was interpreted as the ability of the dye to pass from pre-dyed cells to undyed cells. This was determined by measuring the fluorescence of cells with the FACSCaliber flow cytometer with a 530-nm band pass filter using the technique of Tomasetto *et al.* (*22*). Fluorescent signals were processed over a four-decade logarithmic range. The clusters containing 100% dyed and undyed cells served as positive and negative controls. A no-dye-transfer control for the 50% dyed cell clusters was prepared by mixing equal volumes of the final suspensions of the 100% dyed and undyed cells, and the resulting mixture was immediately analyzed with the flow cytometer.

RESULTS

100% Labeling: Response of Multicellular Clusters and Cell Suspensions

Figure 1 illustrates the surviving fraction of cells maintained in multicellular clusters for 72 h as a function of ^{3}H activity (mBq) per labeled cell. Also shown is the survival curve obtained when cells were prepared identically except for maintenance as a single-cell suspension for 72 h at

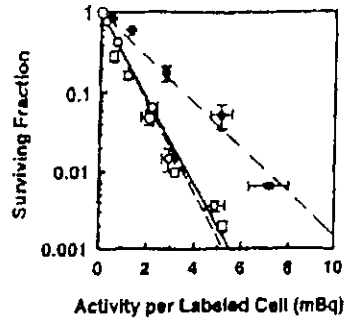

FIG. 1. Survival of V79 cells as a function of activity per labeled cell wherein 100% of the cell population was labeled with [^{3}H]dThd. Cells were maintained in MEMA as multicellular clusters in the absence (○) and presence (●) of 10% DMSO, or as suspensions in the absence of DMSO (□). Data points represent the average of eight (○), three (●) and two (□) experiments, respectively. Standard errors are shown accordingly.

10.5°C [see ref. (*19*) for experimental details]. The data were fitted by least squares to the relationship

$$SF = (1 - b)e^{-A/A_1} + b\, e^{-A/A_2}, \qquad (1)$$

where SF is the surviving fraction, A is the activity per labeled cell, and b, A_1 and A_2 are the fitted parameters. The parameters A_1 and A_2 are analogous to D_0 values for the first and second components, respectively. With $b = 0$ for monoexponential response, the fitted values of A_1 for cluster and suspension are 0.80 ± 0.02 and 0.76 ± 0.04 mBq/cell, respectively. The response of the cells to incorporated [^{3}H]dThd is essentially the same whether the cells are arranged in the form of a cluster or are maintained as a single-cell suspension. Therefore, this suggests that the cells within the cluster do not receive any significant exposure to radiation from their neighbors (i.e. no cross-irradiation).

100% Labeling: Modification of Response by DMSO and Lindane

The surviving fractions of cells in multicellular clusters assembled and maintained in the presence or absence of 10% DMSO are also shown in Fig. 1. A least-squares fit of the data for each treatment condition to Eq. (1) with $b = 0$ gives A_1 values of 1.5 ± 0.08 and 0.80 ± 0.02 mBq/cell for 10% and 0% DMSO, respectively (Table 1). The dose modification factor (DMF), which indicates the degree of protection provided to the labeled cells by 10% DMSO, is expressed by the ratio of A_1 values in the presence and absence of DMSO as follows (*19, 23*):

$$\text{DMF}([^3\text{H}]\text{dThd, 10\% DMSO}) = \frac{A_1\ (\text{with DMSO})}{A_1\ (\text{without DMSO})}. \qquad (2)$$

As shown in Table 1, a DMF value of 1.9 ± 0.12 is obtained, which indicates that 10% DMSO is able to protect V79 cells against lethal damage in clusters when all cells are labeled with [^{3}H]dThd. As reported earlier (*13*), 100 μM lindane did not have any effect on the survival of cells

TABLE 1
Fitted Parameters for Survival Curves and Bystander Modification Factor for Multicellular Clusters

Treatment	Percentage of cells labeled	Number of experiments	b	A_1[a] (mBq/labeled cell)	A_2[a] (mBq/labeled cell)	Bystander modification factor[b]
[³H]dThd	100	8	0	0.80 ± 0.02[c]	—	—
[³H]dThd + 10% DMSO	100	2	0	1.5 ± 0.08	—	1.9 ± 0.12[d]
[³H]dThd	50	4	0.61 ± 0.09	0.29 ± 0.16	4.8 ± 1.1	—
[³H]dThd + 10% DMSO	50	5	0.52 ± 0.08	1.5 ± 0.28	11.1 ± 2.1	2.3 ± 0.68
[³H]dThd + 100 μM lindane	50	3	0.68 ± 0.03	0.72 ± 0.15	18.2 ± 2.0	3.8 ± 0.94
[³H]dThd + 10% DMSO + 100 μM lindane	50	3	0.61 ± 0.03	1.1 ± 0.20	29.5 ± 2.8	6.1 ± 1.5
[³H]dThd	10	2	0.87 ± 0.02	0.96 ± 0.40	49.4 ± 1.9	—
[³H]dThd + 10% DMSO	10	2	0.84 ± 0.02	1.4 ± 0.65	67.0 ± 4.3	1.4 ± 0.10
[³H]dThd + 100 μM lindane	10	2	0.82 ± 0.02	1.4 ± 0.77	91.0 ± 6.7	1.8 ± 0.15
[³H]dThd + 10% DMSO + 100 μM lindane	10	2	0.86 ± 0.03	3.5 ± 1.8	112.4 ± 7.5	2.3 ± 0.17

[a] A_1 and A_2 are analogous to the D_0's of the first (labeled cells) and second (bystander cells) components of the fitted survival curve (Eq. 1).
[b] A_2 (with treatment)/A_2 (without treatment).
[c] Mean ± SE.
[d] For 100% labeling, this quantity represents the traditional dose modification factor (DMF).

from a multicellular cluster when all cells were labeled with [³H]dThd. This suggests that the bystander effect does not significantly contribute to the killing of radiolabeled cells.

50% Labeling: Modification of Response by DMSO and/or Lindane

Figure 2A shows the cell surviving fraction as a function of the level of radioactivity per labeled cell for multicellular clusters in which 50% of the cells were labeled with [³H]dThd. The clusters were maintained in the presence of (1) MEMA, (2) 10% DMSO in MEMA, (3) 100 μM lindane in MEMA, or (4) 10% DMSO + 100 μM lindane in MEMA. As shown in Fig. 2A, a two-component exponential survival curve emerges when the data from each experimental condition are fitted to Eq. (1). As expected, the transition from the first to second component occurs near 50% survival. Table 1 summarizes the fitted parameters for the different treatment conditions. The fitted parameters for cases (1) and (3) are slightly different from those obtained previously (*13*) because the new values include results of additional experiments not reported earlier. In the absence of any treatment, as the activity per labeled cell increases, the surviving fraction drops sharply to about 50% and then continues to drop, albeit with a shallower slope. The first component of the two-component survival curve represents killing of the radiolabeled cells, whereas the second component represents killing of unlabeled bystander cells (*13*). Addition of 10% DMSO afforded significant protection against lethal damage to unlabeled bystander cells. In fact, the value of A_2 changes from 4.8 ± 1.1 to 11.1 ± 2.1 mBq/labeled cell (Table 1). If one considers this change a consequence of modification of the bystander effects imparted by the labeled cells to unlabeled cells, then the bystander modification factor (BMF) is defined as[3]

$$\text{BMF} = \frac{A_2 \text{ (with treatment)}}{A_2 \text{ (without treatment)}}. \qquad (3)$$

The bystander modification factor for 10% DMSO in multicellular clusters containing 50% cells labeled with [³H]dThd is 2.3 ± 0.68 (Table 1). A greater degree of protection of the bystander cells was achieved with 100 μM lindane (bystander modification factor = 3.8 ± 0.94). This value is within statistical uncertainties of the previously reported value of 3.5 ± 1.0 (*13*). The most dramatic protection of the bystander cells was manifested by a combined treatment of 10% DMSO and 100 μM lindane, which yields

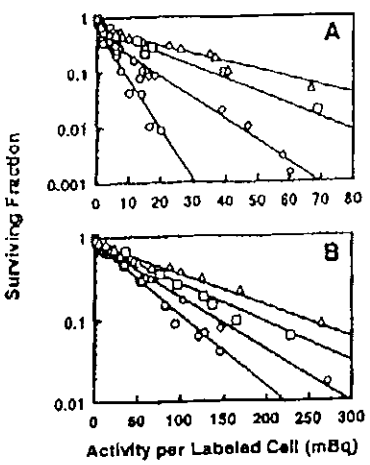

FIG. 2. Survival of V79 cells as a function of activity per labeled cell in which 50% (panel A) or 10% (panel B) of the cells were labeled with [³H]dThd and used to form multicellular clusters. The clusters were maintained in MEMA (○), 10% DMSO in MEMA (◇), 100 μM lindane in MEMA (□), or 10% DMSO + 100 μM lindane in MEMA (△). Data from two to five independent experiments are presented for each treatment. Standard errors for each data point are of the order of the dimensions of the symbols.

[3] In our previous communication, we designated the ratio of the A_2 values as a bystander blocking factor. This name was selected because lindane is a gap junction inhibitor in V79 cells. The change in name to bystander modification factor acknowledges the fact that other agents such as DMSO can modify the response through other mechanisms.

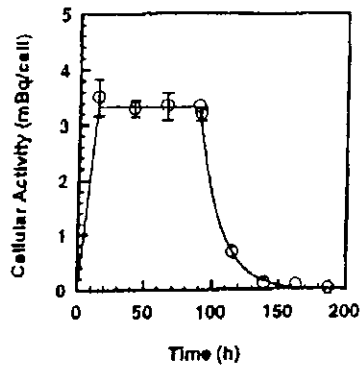

FIG. 3. Intracellular ^{3}H activity in V79 cells as a function of time. The period 0–12 h represents the uptake of the radiochemical. The period 12–84 h represents the 72-h period in which the cells were maintained at 10.5°C. The period beyond 84 h corresponds to the 1-week period of colony formation, when the cellular activity has an effective half-time of ~12 h. The area under the curve is proportional to the cumulative decays in the V79 cell nucleus. Approximately 76% of the intracellular decays occur when the cells were maintained at 10.5°C.

a sharp drop in the response curve to about 50% survival and only limited cell killing at higher activities per labeled cell (Fig. 2A). Under this experimental condition, a bystander modification factor of 6.1 ± 1.5 was obtained.

10% Labeling: Modification of Response by DMSO and/or Lindane

The multicellular clusters were also prepared with a mixture of 10% radiolabeled cells and 90% unlabeled cells. As in the case for 50% labeling, Fig. 2B shows a similar two-component exponential response for each treatment condition. As expected, the transition from the first to second component for 10% labeling occurs near 90% survival. The parameters resulting from least-squares fits to Eq. (1) are given in Table 1. The bystander modification factors corresponding to 10% DMSO, 100 μ*M* lindane, and 10% DMSO + 100 μ*M* lindane are 1.4 ± 0.10, 1.8 ± 0.15, and 2.3 ± 0.17, respectively (Table 1). These values for the case of 10% labeling were of lesser magnitude than those for the 50% labeling. However, like the data for 50% labeling, the data for 10% labeling show that the killing of unlabeled bystander cells does not saturate even though the number of labeled cells that come in contact with unlabeled cells is five times less than in the case of the 50% labeling.

Biokinetics of [^{3}H]dThd in Cells

The uptake, maintenance and clearance of [^{3}H]dThd in V79 cells as they proceed through different stages of the experiment are depicted in Fig. 3. The area under the curve is proportional to the cumulated activity (decays) of ^{3}H in V79 cell nuclei. The period of 0–12 h represents the uptake of the radiochemical at 37°C. Previous studies have shown that the uptake is linear in time during this period (*23*). The period of 12–84 h represents the 72-h period in which the cells were maintained at 10.5°C in the cluster configuration.

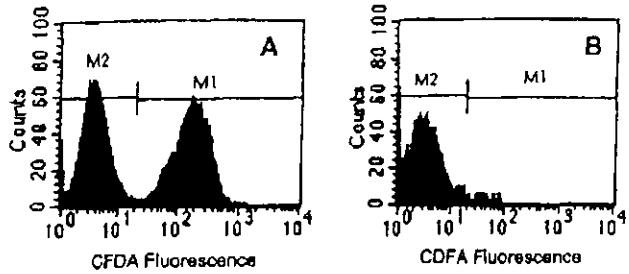

FIG. 4. Evidence of no migration of radioactivity from labeled to unlabeled cells in multicellular cluster containing 50% labeled cells. V79 cells were radiolabeled with [^{3}H]dThd, dyed with CFDA, and mixed with unlabeled and undyed cells, and cell clusters were prepared and maintained at 10.5°C for 72 h. Panel A: After 72 h, flow cytometry analysis shows that 49.6% of the cells remained dyed (M1). Panel B: The undyed cells (M2) were separated from the dyed cells (M1) by FACS. No significant radioactivity was found in the undyed cells.

As expected, the cellular activity did not change during this period. Finally, the curved region corresponds to the 1-week period of colony formation at 37°C, where the cellular activity has an effective half-time of ~12 h, which is in agreement with previous data (*23*). Integration under the curve and normalizing to 1 mBq give the mean cumulated activity (decays) in a labeled cell, $\bar{A}$ = 343 Bq s per mBq in the cell. Finally, it should be noted that about 76% of the intracellular decays occurred while the cells were maintained in the cluster configuration at 10.5°C (*23*).

No Migration of Radioactivity In Multicellular Clusters

The multicellular clusters consisting of 50% radiolabeled and dyed cells and 50% unlabeled and undyed cells were maintained at 10.5°C for 72 h, dispersed, and analyzed by flow cytometry to verify percentage of cells dyed. The analysis of CFDA-positive and CFDA-negative cells is shown in Fig. 4A. The data confirm that 49.6% of the cells were dye-positive (M1 gate) and hence labeled with [^{3}H]dThd. The dye-negative cells (M2 gate) were then sorted and again analyzed by flow cytometry (Fig. 4B). Figure 4B shows that the undyed cells (M2 gate) were separated to a purity of ~97%. Aliquots of these cells were counted for radioactivity, and it was determined that they contained an average of 0.013 mBq/cell. The M1-gated (dye-positive) cells shown in Fig. 4A contained 1.5 mBq/cell. Since the dye-negative cells have a 3% contamination of radiolabeled and dyed cells, this population should have an average of at least 0.045 mBq/cell. This is well above the 0.013 mBq/cell observed. Therefore, these data provide strong evidence that there is no migration of [^{3}H]dThd from radiolabeled cells to surrounding unlabeled cells under the experimental conditions used.

Absorbed Dose to Labeled and Unlabeled Cells

The short-range β particles emitted by ^{3}H have a spectrum of energies from 0–18.6 keV (*24*), with ranges in water from 0–7 μm. The mean energy of the electron is only

5.7 keV, and it has a range of 1 μm in water. The mean diameter of a V79 cell is 10 μm, and the mean diameter of its nucleus is 8 μm (*25*). Using the model of Goddu *et al.* (*26*) and the full ^{3}H β-particle spectrum, the mean self-absorbed dose to the nucleus of a labeled cell per unit cumulated activity in the nucleus of the labeled cell is S_{self}(labeled←labeled) = 2.61 × 10^{-3} Gy/Bq s. The mean self-absorbed dose to the nucleus, D_{self}(labeled), is $\tilde{A}$ S_{self}(labeled←labeled) = 0.895 Gy per mBq in the cell. Therefore, the mean lethal dose for 100% labeling is D_{37} = 0.80 mBq (0.895 Gy/mBq) = 0.72 Gy. In contrast, the mean cross-dose to a neighboring unlabeled cell per unit cumulated activity in a single labeled cell is S_{cross}(unlabeled←labeled) = 3.03 × 10^{-6} Gy/Bq s. For 50% labeling, each unlabeled cell has 12 neighbors, 6 of which are labeled (*26*). Therefore, S^{total}_{cross}(unlabeled←labeled) = 1.82 × 10^{-5} Gy/Bq s and D^{total}_{cross}(unlabeled←labeled) = 0.00624 Gy mBq^{-1} in the labeled cell. Therefore, the dose to the labeled cell is over 140 times that to the unlabeled cell.

Functional GJIC in Multicellular Clusters

The fluorescent dye calcein AM was used to ascertain the presence of functional GJIC. As shown in Fig. 5A, the background fluorescence associated with undyed cells resulted in a single low-intensity peak with a geometric mean of 2.9. When 100% of the cells were dyed, a single broad and intense peak was observed with a geometric mean of 290 (Fig. 5B). When 50% of the cells were loaded with the dye, two peaks emerged with geometric means of 13 and 203, respectively (Fig. 5C). The peak corresponding to initially undyed cells has shifted markedly to the right, indicating that dye has been transferred from dyed to undyed cells. Hence functional GJIC is present in the V79 multicellular clusters maintained at 10.5°C. Addition of lindane inhibited dye transfer, as shown by the similarity of its histogram (Fig. 5D, geometric means of 9 and 225) to that of the 50% control culture, where no dye transfer was possible (Fig. 5E, geometric means of 6 and 260). These data support the capacity of lindane to attenuate GJIC under the present experimental conditions.

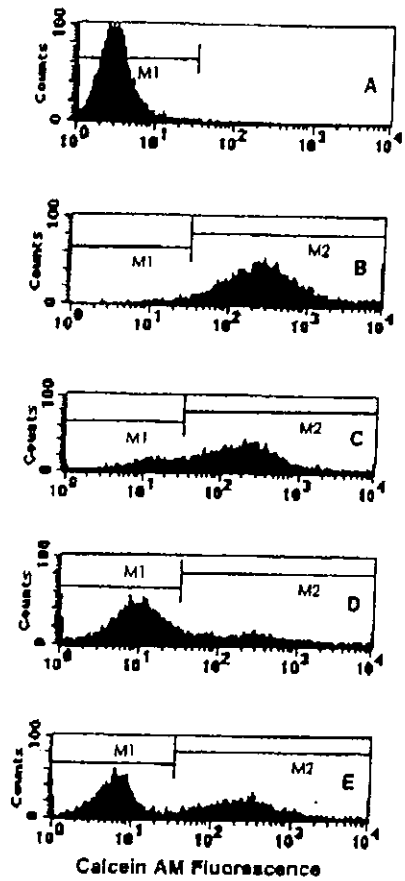

FIG. 5. Single-parameter histogram from flow cytometry of V79 cells from a multicellular cluster containing (panel A) 0%, (panel B) 100% or (panel C) 50% dyed cells. (panel D) 50% dyed cells in the presence of 100 μ*M* lindane, or (panel E) an equal mixture of 0% and 100% dyed cells followed by immediate analysis. Transfer of the fluorescent dye calcein AM from dyed to undyed cells in the case of 50% dyed cells is seen in the right lateral shift in the peak position corresponding to the cells that were initially undyed (panel C). Addition of lindane dramatically reduces the degree of dye transfer (panel D) as seen in the similarity to the 50% control histogram, where no dye transfer was possible (panel E).

DISCUSSION

The present study has used a three-dimensional tissue culture model (*13*) to quantify the lethal effect of nonuniform distributions of [^{3}H]dThd. This model affords a high degree of control over the percentage of radiolabeled cells in the cluster. The short range of the ^{3}H β particles prevents significant irradiation of unlabeled cells by radioactivity in the labeled cells (*13*). This is supported by the data in Fig. 1 that show that the mean lethal ^{3}H activity per cell required to achieve 37% survival is essentially the same for 100% labeling regardless of whether the cells are maintained as clusters (0.80 ± 0.02 mBq/cell) or in suspension, where no cross-dose is possible (0.76 ± 0.04 mBq/cell). It is also supported by theoretical calculations for 50% labeling (see Results section) that yield mean absorbed doses to the labeled and unlabeled cells of 0.895 and 0.00624 Gy mBq^{-1} per labeled cell, respectively. Since the activity per labeled cell required to effect 1% survival is about 20 mBq per labeled cell (Fig. 2A), the dose to the unlabeled cells in this case would be about 0.12 Gy. Assuming an equal effectiveness per gray between self- and cross-irradiation (worst-case scenario), this would produce an SF of 0.84 in the unlabeled cells which comprise 50% of the population. If all of the labeled cells were killed, and the killing of unlabeled cells was due to irradiation of their nuclei, this would yield an expected SF for the entire population of about 0.42. Similar results emerge for the case of 10% labeling. The difference between 0.42 and the observed SF of 0.01 suggests that mechanisms other than cross-irradia-

tion play the principal role in the observed killing of unlabeled bystander cells.

Three different radiolabeling conditions were investigated in which 100, 50 or 10% of the cells within the multicellular clusters were labeled, each resulting in markedly different survival curves. The data for 100% labeling in Fig. 1 yielded an exponential survival curve with a mean lethal cellular activity of 0.80 mBq/cell. In contrast, the data for 50 and 10% labeling required fits to a two-component exponential function (Fig. 2A, B). These fits and the resulting parameters (Table 1) indicate that about 50 and 10% of the cells are killed at relatively low activities per labeled cell because only the labeled cells are killed. However, the second components (Fig. 2) indicate that unlabeled cells are killed even though they do not receive significant irradiation. This strongly suggests that bystander effects are responsible for killing of unlabeled cells. Furthermore, the linearity of the second components suggests that the bystander signal increases exponentially with the dose to the labeled (irradiated) cells. This finding appears to differ from the data of Wu *et al.* (*27*), who found a saturation in the dose response for mutation induction in A_L cells irradiated through the cytoplasm with an α-particle microbeam. They observed a similar saturation in response when cell survival was used as the end point (data available only down to about 70% survival). They postulated that the saturation after eight α-particle traversals may have been due to the fact that the traversals were split between only two areas in the cytoplasm (*27*), suggesting that a more uniform irradiation of the cytoplasm may have eliminated the saturation. While this may be the case, the present data do not involve irradiation of the cytoplasm of the same cell; rather they involve death of unlabeled bystander cells adjacent to cells whose nucleus is irradiated by β particles emitted by [^{3}H]dThd. Therefore, given the very different irradiation conditions (cytoplasm of the same cell compared to the nucleus of a neighboring cell), it is possible that different mechanisms are operational, which could lead to different dose–response relationships. Furthermore, considering other differences between the experimental protocols (e.g. radiation type, cell type, dose of radiation to target cells, temperature, cell geometry), it is not surprising that differences were observed.

A more recent report from the same laboratory examined the mutagenic response in the surviving bystander cell population after irradiation of 0, 5, 10 or 20% of the cell nuclei with 20 α particles from the microbeam (*28*). Under these irradiation conditions, which were somewhat similar to those in the present study, they found a linear increase in the mutant fraction of bystander cells as the percentage of cell nuclei in the population that were hit with the 20 α particles was increased. A plateau was reached when 10% of the nuclei were hit such that there was no significant difference in mutation fraction when 20% of the cells in the population were hit. As indicated by the authors, this was perhaps expected in their two-dimensional monolayer model because the number of unirradiated cells in direct contact with an irradiated cell is not much different in the two cases. The data in the present work also suggest that percentage of cells labeled is an important determinant for bystander effects. However, in the present work, higher percentages of labeling appear to impart bystander effects more efficiently in the three-dimensional cluster model. The fitted values for A_2 (Table 1) differ by about 10-fold for 10% and 50% labeling, despite only a 5-fold difference in the percentage of cells labeled. Therefore, the efficiency of the transfer of bystander effects is reduced by a factor of two for 10% labeling compared to 50% labeling. It is possible that coupling of an average of about 1.2 radioactive cells to each bystander cell (10% labeling) results in transmission of damage signals to a single region of the bystander cell compared to a more uniform transmission when 6 radioactive cells are coupled to each bystander cell (50% labeling). This could lead to less efficient killing of the coupled bystander cell. Although we are not aware of any experimental data to support this hypothesis, this argument is analogous to that of Wu *et al.* (*27*) for cytoplasmic irradiation.

Gap junctional intercellular communication has been implicated as an important mediator of radiation-induced bystander effects (*6*). Gap junctions are intercellular membrane channels that directly link the interiors of neighboring cells. These channels have diameters of 1.5–2 nm and permit the direct passage of small (<2,000 Da) molecules between the cytoplasm of neighboring cells (*29*). V79 cells were reported to have some GJIC at physiological temperature (*16–18, 30*). It has also been shown by scrape-loading and dye transfer that V79 cells retained GJIC even when maintained for 72 h at 10.5°C as a confluent monolayer (*13*). While this served as evidence of GJIC in monolayers at 10.5°C, it was necessary to demonstrate the presence of functional coupling of V79 cells in multicellular clusters maintained at 10.5°C. This was studied in the present work by monitoring the transfer of the fluorescent dye calcein AM, which can traverse gap junctions, by flow cytometry. Figure 5 shows that functional gap junctions are indeed formed between the neighboring cells within the cluster, as shown by the transfer of calcein AM from dyed to undyed cells. Moreover, the current study also shows that GJIC between V79 cells in the multicellular cluster can be inhibited to some degree by lindane. This is in agreement with earlier findings (*17, 31*). It is perhaps not surprising that functional coupling occurs at 10.5°C. Ward *et al.* (*32*) have shown that V79 cells are able to repair DNA single-strand breaks at 10°C, albeit at a reduced rate. Double-strand breaks were not repaired at this temperature. Therefore, while 10.5°C does not represent normal body temperature, many important physiological processes such as repair and GJIC remain operational.

To elucidate the potential mechanisms responsible for bystander effects observed with 50 and 10% labeling, DMSO and/or lindane was added to the culture medium

before the multicellular clusters were formed. Our results show that 10% DMSO offered a fair degree of protection of bystander cells in both labeling situations (Table 1). A better protective effect was afforded by 100 μ*M* lindane. However, concurrent treatment with DMSO and lindane brought about maximum protection of the bystander cells. For 50% labeling, the effect of a combined treatment was more prominent than for 10%, with bystander modification factor values of 6.1 ± 1.5 and 2.3 ± 0.17, respectively. This difference may be explained in light of the interactions between the labeled and unlabeled cells. The metabolic generation of ROS due to oxidative stress after exposure to ionizing radiation has recently been hypothesized as a mediator of bystander responses in unirradiated cells (*10, 33*). Exposure to high concentrations of ROS results in a wide spectrum of DNA damage, cell cycle arrest, senescence, and eventually cell death (*1, 34–36*). In the present study, significant protection (DMF = 1.9 ± 0.12) was afforded by DMSO against killing of cells in multicellular clusters in which 100% of the cells were labeled. The intracellular generation of ·OH by ^{3}H decays may be the principal cause of cell death. DMSO is a potent scavenger of ·OH (*37*), and it is therefore expected to attenuate the effect of [^{3}H]dThd provided that an adequate concentration of DMSO is used (*19*). However, ·OH are short-lived and can diffuse only about 4 nm (*38*). Thus, while these ·OH may account for lethal damage to labeled cells in the case of 100% labeling, no transmissible lethality to unlabeled bystander cells should occur with this source of ·OH. However, it is possible that there could be more persistent production of ·OH from another source such as superoxide ($O_2^{\cdot-}$) (*10, 39*). It is possible that free radicals, particularly ·OH, produced through these mechanisms could lead to membrane lipid peroxidation and consequent formation of a number of free radicals capable of producing DNA damage and cell death (*40–42*). While DMSO could block some of the above events in labeled cells and thereby reduce the concentration of free radicals in bystander cells, it is possible that some of the long-lived radicals that are not scavenged by DMSO may escape through gap junctions, reach the neighboring cells, and subsequently inflict lethal damage on these cells. The ability of lindane to block gap junctions may prevent the radicals from reacting with the DNA of bystander cells. However, lindane may not entirely abolish GJIC and provide complete protection against damage to the bystander cells by ROS originating in the labeled cells. This is likely in view of the fact that lindane affects GJIC by altering the permeability of gap junction channels and the number of gap junctions (*16, 43*). Further support for this is provided by the data in Fig. 5D, which shows that GJIC-mediated dye transfer was not completely blocked by lindane. Based on the above arguments, the presence of both DMSO and lindane might be expected to have an impact on both the ·OH-initiated events in the labeled cells and their propagation through gap junctions to the bystander cells. This may explain why the bystander modification factor is greater for the combined treatment with DMSO and lindane compared to treatment with either agent alone (Table 1).

Our results with lindane indicating the involvement of GJIC in bystander effects caused by nonuniform distributions of incorporated radioactivity are consistent with those of Azzam *et al.* (*6*), who reported a similar reduction of α-particle-induced bystander effects in human diploid fibroblast cell population by lindane. Recently, Zhou *et al.* (*28*) have provided evidence that irradiation of human–hamster A_L cells induces a bystander mutagenic response in unirradiated neighboring cells that can be inhibited by lindane but not by DMSO. They concluded that a signal transduction pathway other than ·OH-mediated oxidative stress might play a role in mediating the bystander responses for α particles. Although the present study with β particles implicates ·OH as the primary oxidant species responsible for the initiation of damage to bystander cells, it is also possible that other signaling mechanisms triggered by ROS may be involved as proposed by Iyer and Lehnert (*12*). In this context, it should be mentioned that oxidative stress has been correlated with the induction of signal transduction that is linked to a variety of deleterious effects of radiation (*34, 44–46*).

In conclusion, the present study provides new data on the biological effects of nonuniform distributions of incorporated radioactivity using a novel approach to specifically control the degree of nonuniformity. This study also establishes the response of V79 multicellular clusters to incorporated radioactivity and furnishes substantial evidence that bystander effects play a significant role in determining the biological effect of incorporated radioactivity. Furthermore, these data suggest that at least a part of the observed bystander effects are initiated by free radicals and mediated through gap junctions. These findings may ultimately enhance our capacity to predict the biological response of tumor and normal tissue in nuclear medicine and from environmental exposure to radioactivity.

ACKNOWLEDGMENTS

The authors greatly appreciate the insightful comments and suggestions provided by Drs. Edouard I. Azzam and Sonia M. de Toledo, Department of Radiology, UMDNJ–New Jersey Medical School. We are also thankful to Thomas N. Denny for providing access to the FACS. This work was supported in part by USPHS Grant Nos. R01 CA83838 (RWH) and shared instrumentation grant 1 S10 RR14753-01 (TND).

Received: July 17, 2000; accepted: October 6, 2000

REFERENCES

1. R. Iyer and B. E. Lehnert, Effects of ionizing radiation in targeted and nontargeted cells. *Arch. Biochem. Biophys.* 376, 14–25 (2000).
2. H. Nagasawa and J. B. Little, Induction of sister chromatid exchanges by extremely low doses of alpha-particles. *Cancer Res.* 52, 6394–6396 (1992).
3. H. Nagasawa and J. B. Little, Unexpected sensitivity to the induction

of mutations by very low doses of alpha-particle irradiation: Evidence for a bystander effect. *Radiat. Res.* **152**, 552–557 (1999).

4. A. Deshpande, E. H. Goodwin, S. M. Bailey, B. L. Marrone and B. E. Lehnert, Alpha-particle-induced sister chromatid exchange in normal human lung fibroblasts: Evidence for an extranuclear target. *Radiat. Res.* **145**, 260–267 (1996).
5. A. W. Hickman, R. J. Jaramillo, J. F. Lechner and N. F. Johnson, Alpha-particle-induced p53 protein expression in a rat lung epithelial cell strain. *Cancer Res.* **54**, 5797–5800 (1994).
6. E. I. Azzam, S. M. de Toledo, T. Gooding and J. B. Little, Intercellular communication is involved in the bystander regulation of gene expression in human cells exposed to very low fluences of alpha particles. *Radiat. Res.* **150**, 497–504 (1998).
7. K. M. Prise, O. V. Belyakov, M. Folkard and B. D. Michael, Studies on bystander effects in human fibroblasts using a charged particle microbeam. *Int. J. Radiat. Biol.* **74**, 793–798 (1998).
8. C. Mothersill and C. Seymour, Medium from irradiated human epithelial cells but not human fibroblasts reduces the clonogenic survival of unirradiated cells. *Int. J. Radiat. Biol.* **71**, 421–427 (1997).
9. B. E. Lehnert and E. H. Goodwin, Extracellular factor(s) following exposure to alpha particles can cause sister chromatid exchanges in normal human cells. *Cancer Res.* **57**, 2164–2171 (1997).
10. P. K. Narayanan, E. H. Goodwin and B. E. Lehnert, Alpha particles initiate biological production of superoxide anions and hydrogen peroxide in human cells. *Cancer Res.* **57**, 3963–3971 (1997).
11. P. K. Narayanan, K. E. A. LaRue, E. H. Goodwin and B. E. Lehnert, Alpha particles induce the production of interleukin-8 by human cells. *Radiat. Res.* **152**, 57–63 (1999).
12. R. Iyer and B. E. Lehnert, Factors underlying the cell growth-related bystander responses to alpha particles. *Cancer Res.* **60**, 1290–1298 (2000).
13. A. Bishayee, D. V. Rao and R. W. Howell, Evidence for pronounced bystander effects caused by nonuniform distributions of radioactivity using a novel three-dimensional tissue culture model. *Radiat. Res.* **152**, 88–97 (1999).
14. C. Mothersill and C. B. Seymour, Cell–cell contact during gamma irradiation is not required to induce a bystander effect in normal kidney keratinocytes: Evidence for release during irradiation of a signal controlling survival into the medium. *Radiat. Res.* **149**, 252–262 (1998).
15. G. Kroemer, The proto-oncogene Bcl-2 and its role in regulating apoptosis. *Nat. Med.* **3**, 614–620 (1997).
16. S. B. Yancey, J. E. Edens, J. E. Trosko, C. C. Chang and J. P. Revel, Decreased incidence of gap junctions between Chinese hamster V-79 cells upon exposure to the tumor promoter 12-*o*-tetradecanoyl phorbol-13-acetate. *Exp. Cell Res.* **139**, 329–340 (1982).
17. M. H. El-Fouly, J. E. Trosko and C. C. Chang, Scrape-loading and dye transfer: A rapid and simple technique to study gap junctional intercellular communication. *Exp. Cell. Res.* **168**, 422–430 (1987).
18. H. Banrud, S. O. Mikalsen, K. Berg and J. Moan, Effects of ultraviolet radiation on intercellular communication in V79 Chinese hamster fibroblasts. *Carcinogenesis* **15**, 233–239 (1994).
19. A. Bishayee, D. V. Rao, L. G. Bouchet, W. E. Bolch and R. W. Howell, Radioprotection by DMSO against cell death caused by intracellularly localized iodine-125, iodine-131 and polonium-210. *Radiat. Res.* **153**, 416–427 (2000).
20. G. S. Goldberg, J. F. Beckherger and C. C. G. Naus, A pre-loading method of evaluating gap junctional communication by fluorescent dye transfer. *BioTechniques* **18**, 490–497 (1995).
21. W. Zhang, W. T. Couldwell, M. F. Simard, H. Song, J. H. C. Lin and M. Nedergaard, Direct gap junction communication between malignant glioma cells and astrocytes. *Cancer Res.* **59**, 1994–2003 (1999).
22. C. Tomasetto, M. J. Nepeu, J. Daley, P. K. Horan and R. Sager, Specificity of gap junction communication among human mammary cells and connexin transfectants in culture. *J. Cell Biol.* **122**, 157–167 (1993).
23. R. W. Howell, S. M. Goddu, A. Bishayee and D. V. Rao, Radioprotection against lethal damage caused by chronic irradiation with radionuclides *in vitro*. *Radiat. Res.* **150**, 391–399 (1998).
24. E. Browne and R. B. Firestone, *Table of Radioactive Isotopes*. Wiley, New York, 1986.
25. R. W. Howell, D. V. Rao, D-Y. Hou, V. R. Narra and K. S. R. Sastry, The question of relative biological effectiveness and quality factor for Auger emitters incorporated into proliferating mammalian cells. *Radiat. Res.* **128**, 282–292 (1991).
26. S. M. Goddu, D. V. Rao and R. W. Howell, Multicellular dosimetry for micrometastases: Dependence of self-dose versus cross-dose to cell nuclei on type and energy of radiation and subcellular distribution of radionuclides. *J. Nucl. Med.* **35**, 521–530 (1994).
27. L. J. Wu, G. R. Randers-Pehrson, A. Xu, C. A. Waldren, C. R. Geard, Z. L. Yu and T. K. Hei, Targeted cytoplasmic irradiation with alpha particles induces mutations in mammalian cells. *Proc. Natl. Acad. Sci. USA* **96**, 4959–4964 (1999).
28. H. Zhou, G. Randers-Pehrson, C. A. Waldren, D. Vannais, E. J. Hall and T. K. Hei, Induction of a bystander mutagenic effect of alpha particles in mammalian cells. *Proc. Natl. Acad. Sci. USA* **97**, 2099–2104 (2000).
29. J. E. Trosko and R. J. Ruch, Cell–cell communication in carcinogenesis. *Front. Biosci.* **3**, 208–236 (1998).
30. M. J. Zeilmaker and H. Yamasaki, Inhibition of junctional intercellular communication as a possible short-term test to detect tumor-promoting agents: Results with nine chemicals tested by dye transfer assay in Chinese hamster V79 cells. *Cancer Res.* **46**, 6180–6186 (1986).
31. G. Tsushimoto, C. C. Chang, J. E. Trosko and F. Matsumura, Cytotoxicity, mutagenic, and cell–cell communication inhibitory properties of DDT, lindane, and chlordane on hamster cells *in vitro*. *Arch. Environ. Contam. Toxicol.* **12**, 721–730 (1983).
32. J. F. Ward, C. L. Limoli, P. M. Calabro-Jones and J. Aguilera, An examination of the repair saturation hypothesis for describing shouldered survival curves. *Radiat. Res.* **127**, 90–96 (1991).
33. S. M. Clutton, K. M. S. Townsend, C. Walker, J. D. Ansell and E. G. Wright, Radiation-induced genomic instability and persisting oxidative stress in primary bone marrow cultures. *Carcinogenesis* **17**, 1633–1639 (1996).
34. Q. Chen and B. N. Ames, Senescence-like growth arrest induced by hydrogen peroxide in human diploid fibroblast F65 cells. *Proc. Natl. Acad. Sci. USA* **91**, 4130–4134 (1994).
35. G. McLennan, L. W. Oberley and A. Autor, The role of oxygen-derived free radicals in radiation-induced damage and death of non-dividing eukaryotic cells. *Radiat. Res.* **84**, 122–132 (1980).
36. J. E. Spencer, A. Jenner, O. I. Aruoma, C. E. Cross, R. Wu and B. Halliwell, Oxidative DNA damage in human respiratory tract epithelial cells: Time course in relation to DNA strand breakage. *Biochem. Biophys. Res. Commun.* **224**, 17–22 (1996).
37. M. R. Raju, M. E. Schillachi, S. G. Carpenter, D. T. Goodhead and J. F. Ward, Radiobiology of ultrasoft X rays. V. Modification of cell inactivation by dimethyl sulfoxide. *Radiat. Res.* **145**, 563–567 (1996).
38. R. Roots and S. Okada, Protection of DNA molecules of cultured mammalian cells from radiation-induced single-strand scissions by various alcohols and SH compounds. *Int. J. Radiat. Biol.* **21**, 329–342 (1972).
39. P. A. Riley, Free radicals in biology: Oxidative stress and the effects of ionizing radiation. *Int. J. Radiat. Biol.* **65**, 27–33 (1994).
40. B. Peter, M. Wartena, H. H. Kampinga and A. W. T. Konings, Role of lipid peroxidation and DNA damage in paraquat toxicity and the interaction of paraquat with ionizing radiation. *Biochem. Pharmacol.* **43**, 705–715 (1992).
41. C. L. Limoli, A. Hartmann, L. Shephard, C. Yang, D. A. Boothman, J. Bartholomew and W. F. Morgan, Apoptosis, reproductive failure, and oxidative stress in Chinese hamster ovary cells with compromised genomic integrity. *Cancer Res.* **58**, 3712–3718 (1998).
42. Y. Higuchi and S. Matsukawa, Glutathione depletion induces giant DNA and high-molecular-weight DNA fragmentation associated with

apoptosis through lipid peroxidation and protein kinase C activation in C6 glioma cells. *Arch. Biochem. Biophys.* **363**, 33–42 (1999).

43. X. Guan, W. J. Bonney and R. J. Ruch, Changes in gap junction permeability, gap junction number, and connexin43 expression in lindane-treated rat liver epithelial cells. *Toxicol. Appl. Pharmacol.* **130**, 79–86 (1995).

44. J. E. Trosko and T. Inoue, Oxidative stress, signal transduction, and intercellular communication in radiation carcinogenesis. *Stem Cells* **15** (Suppl. 2), 59–67 (1997).

45. R. H. Burdon, Superoxide and hydrogen peroxide in relation to mammalian cell proliferation. *Free Radic. Biol. Med.* **18**, 775–795 (1995).

46. J. Remacle, M. Raes, O. Toussaint, P. Renard and G. Rao, Low levels of reactive oxygen species as modulators of cell function. *Mutat. Res.* **316**, 103–122 (1995).

Research Article

Assessment of Low Linear Energy Transfer Radiation–Induced Bystander Mutagenesis in a Three-Dimensional Culture Model

Rudranath Persaud, Hongning Zhou, Sarah E. Baker, Tom K. Hei, and Eric J. Hall

Center for Radiological Research, Columbia University Medical Center, New York, New York

Abstract

A three-dimensional cell culture model composed of human-hamster hybrid (A_L) and Chinese hamster ovary (CHO) cells in multicellular clusters was used to investigate low linear energy transfer (LET) radiation–induced bystander genotoxicity. CHO cells were mixed with A_L cells in a 1:5 ratio and briefly centrifuged to produce a spheroid of 4×10^6 cells. CHO cells were labeled with tritiated thymidine ([^{3}H]dTTP) for 12 hours and subsequently incubated with A_L cells for 24 hours at 11°C. The short-range β-particles emitted by [^{3}H]dTTP result in self-irradiation of labeled CHO cells; thus, biological effects on neighboring A_L cells can be attributed to the bystander response. Nonlabeled bystander A_L cells were isolated from among labeled CHO cells by using a magnetic separation technique. Treatment of CHO cells with 100 μCi [^{3}H]dTTP resulted in a 14-fold increase in bystander mutation incidence among neighboring A_L cells compared with controls. Multiplex PCR analysis revealed the types of mutants to be significantly different from those of spontaneous origin. The free radical scavenger DMSO or the gap junction inhibitor Lindane within the clusters significantly reduced the mutation incidence. The use of A_L cells that are dominant negative for connexin 43 and lack gap junction formation produced a complete attenuation of the bystander mutagenic response. These data provide evidence that low LET radiation can induce bystander mutagenesis in a three-dimensional model and that reactive oxygen species and intercellular communication may have a modulating role. The results of this study will address the relevant issues of actual target size and radiation quality and are likely to have a significant effect on our current understanding of radiation risk assessment. (Cancer Res 2005; 65(21): 9876-82)

Introduction

The radiation-induced "bystander effect" refers to the induction of biological effects in cells that are not directly traversed by a charged particle but are in close proximity to cells that are. The bystander effect has been shown for a variety of end points, such as micronucleus induction, cell lethality, gene expression, and oncogenic transformation, by using a range of rodent and human cell culture models, but most studies have involved high linear energy transfer (LET) α-particles (1). There is clearly a need to ascertain whether a similar response can be observed with low LET radiation at doses correlating to environmental exposure.

There is evidence that low LET radiation can induce a cytotoxic bystander response in mammalian cells (2, 3). By using DMSO and Lindane as modulators, Bishayee et al. (4, 5) have shown that bystander cytotoxicity is free radical initiated and gap junction mediated, respectively. Furthermore, there is evidence that damage to cells from short-range β-particles resulted in an enhanced transformation yield among cells in close proximity by a factor of 10 compared with cells not in contact with damaged cells (6). In addition, X-rays delivered by a microbeam that targeted a single cell in a population produced bystander cell cytotoxicity that was similar to that when all the cells were exposed (7). Studies have also investigated the direct effects of low LET radiation where the entire population of cells was targeted and subsequently evaluated. Low LET protons were found to produce cytotoxicity, micronuclei induction, CD59 mutations, hypoxanthine phosphoribosyltransferase mutations, and chromosomal aberrations (8–11).

Evidence for a bystander response based on *in vivo* studies are rather limited. By evaluating tumor growth in mice, a significant growth inhibitory effect was observed within the nonirradiated, bystander tumor cell population adjacent to neighboring ^{3}H-labeled tumor cells emitting short-range β-particles (12). By using exogenous neutron-irradiated bone marrow cells implanted in mice, the progeny was determined to exhibit chromosomal instability (13). The present study uses a heterogeneous three-dimensional multicellular model that can mimic a tissue microenvironment and thereby provide important information on the relevance of the bystander effect to *in vivo* conditions.

Many bystander studies with low LET radiation involve the analysis of the cells as one population and not separately as directly labeled/irradiated compared with the unlabeled/nonirradiated bystander cells. This study separated and isolated the directly labeled Chinese hamster ovary (CHO) cells from the neighboring nonlabeled bystander A_L cells within the clusters. This allows for the most effective evaluation of the bystander response because the bystander A_L cell population can be studied independently for cytotoxicity and mutagenesis. The human-hamster hybrid A_L cells used in this study contain a full set of hamster chromosomes and a single copy of human chromosome 11, which includes the *CD59* gene that encodes for the CD59 cell surface antigen. Mutants ($CD59^-$) can be detected and scored with the use of a complement-mediated cytotoxicity assay that uses the E7.1 monoclonal antibody against the CD59 antigen to destroy wild-type $CD59^+$ cells while sparing $CD59^-$ cells that subsequently proliferate to form mutant colonies. The mutation spectra of such mutants can be determined with great specificity because mutations are detectable that range in size from a single base pair to chromosomal mutations involving the loss of the entire human chromosome 11.

The demonstration of low LET radiation–induced bystander mutagenesis in a cell culture model that represents *in vivo* conditions may influence the calculations involved in risk assessment. This could subsequently result in changes in risk management for low LET radiation exposure. This study was undertaken to show

Requests for reprints: Eric J. Hall, Center for Radiological Research, Columbia University Medical Center, 630 West 168th Street, New York, NY 10032. Phone: 212-305-5660; Fax: 212-305-3229; E-mail: ejh1@columbia.edu.

doi:10.1158/0008-5472.CAN-04-2875

a correlation between low LET radiation and bystander mutagenicity in a three-dimensional cell culture model and to implicate the roles of reactive oxygen species and gap junctional intercellular communication in the bystander response.

Materials and Methods

Cell culture. For this study, human-hamster hybrid (A_L) and CHO cells were used. The A_L cells contain a standard set of Chinese hamster ovary-K1 chromosomes and a single copy of human chromosome 11 (14). Human chromosome 11 encodes for the CD59 cell surface antigen, and both the chromosome and the antigen can be used effectively in the separation and identification of A_L cells in a mixture with other cell types. Cultures were maintained in Ham's F-12 medium supplemented with 8% heat-inactivated fetal bovine serum, 25 μg/mL gentamicin, and 2× normal glycine (2×10^{-4} mol/L) at 37°C in a humidified 5% CO_2 incubator.

Radiochemical labeling of Chinese hamster ovary cells and preparation of multicellular clusters with A_L cells. Both 8×10^5 A_L and 8×10^5 CHO cells were preconditioned in 1 mL medium in 17 × 100 mm Falcon polypropylene culture tubes on a rocker-roller and incubated for 3 hours. Subsequently, 1 mL medium containing tritiated thymidine ([^{3}H]dTTP; Perkin-Elmer, Boston, MA) was added to the tubes containing CHO cells to produce various activities of the radionuclide. Tubes with control CHO or A_L cells received 1 mL medium. All tubes were incubated for 12 hours after which they were washed thrice with medium to remove excess [^{3}H]dTTP from labeled CHO cells. Four tubes of unlabeled A_L cells were incorporated into one tube of radiolabeled CHO cells to produce a mixture with a total of 4×10^6 cells that resulted in a ratio of 1:5 of radiolabeled CHO cells to unlabeled A_L cells. The cell mixture was centrifuged to produce a pellet and transferred in 0.4 mL medium to a sterile 500 μL microcentrifuge tube. This tube was centrifuged at 1,000 rpm for 1 minute to produce a cluster.

Separation of A_L and Chinese hamster ovary cell clusters by magnetic cell separation. Clusters were maintained at 11°C for 24 hours to allow self-irradiation of CHO cells and possible traversal of any bystander signals to neighboring A_L cells. After exposure, the supernatant was carefully removed and discarded. The clusters were dispersed, transferred to 17 × 100 mm Falcon polypropylene culture tubes, and washed in PBS/EDTA buffer. The cell mixtures were treated for 30 minutes at 4°C with a primary CD59 antibody (Serotec, Inc., Raleigh, NC) that binds the cell surface antigen on A_L cells. Magnetic beads, coated with rabbit anti-mouse IgG that acts as a secondary antibody to the monoclonal CD59 antibody, were incorporated into the cell mixtures and incubated at 4°C for 15 minutes. The cell mixtures were then passed twice through separation columns between magnets (Miltenyi Biotec, Auburn, CA). The effluent contained the unbound CHO fractions, whereas the A_L portions remained in the columns. The columns were removed from between the magnets and the A_L cells were flushed with the aid of a plunger.

Flow cytometric analysis of the separated fractions of Chinese hamster ovary and A_L cells. After incubation of A_L and CHO cells in clusters, magnetic separation was used to isolate two independent populations. To establish whether the separation was proficient, analyses on various mixtures of A_L and CHO cells were done to determine the efficiency of the magnetic separation. This was achieved by using flow cytometric analysis that specifically identifies a FITC tag on the A_L cells. To prepare the cells for such analysis, FITC-conjugated microbeads, as secondary antibodies to the CD59 primary antibody, were used during the separation. The immunophenotypical quantification of A_L cells in each population was done with the use of a FACSCalibur flow cytometer (BD Biosciences, San Jose, CA).

Role of free radicals and intercellular communication. To investigate the role of free radicals, and cell-to-cell communication in bystander mutagenesis, the radical scavenger DMSO (J.T. Baker, Phillipsburg, NJ) and the gap junction inhibitor Lindane (Sigma Chemical Co., St. Louis, MO) were used, respectively. DMSO was used as a 0.2% mixture with medium, and Lindane was used at a concentration of 40 μmol/L. Before the formation of multicellular clusters, cells were washed with medium containing either DMSO or Lindane and clusters were generated. To eliminate the indirect effects of Lindane, connexin 43–deficient A_L cells (DN6) that lack functional gap junctions were used in the cluster. Cells (CXV2) containing the empty vector were used as their controls.

Functional gap junction formation between Chinese hamster ovary and A_L cells. To show that intercellular communication was operational between A_L and CHO cells within the three-dimensional model, transfer of the dye Calcein M (Molecular Probes, Boston, MA) from CHO to A_L cells was determined. Briefly, 8×10^5 CHO cells were incubated with 20 μmol/L Calcein M for 25 minutes and washed twice with PBS to remove excess dye. The cells were resuspended in medium and incubated for 30 minutes. Control and nondyed cells were treated the same. CHO cells were combined with 3.2×10^6 A_L cells, centrifuged to produce a cluster, and incubated for 24 hours at 11°C. This temperature was chosen to reduce the metabolic rate of the cells, thereby allowing them to survive in the spheroid formation. The cluster was resuspended in fluorescence-activated cell sorting buffer and the extent of dye migration was determined by a FACSCalibur flow cytometer.

Dose response for cell cytotoxicity. After the magnetic separation of the clusters into A_L and CHO fractions, cells were counted by using a hemocytometer and then plated into 100 mm diameter Petri dishes for colony formation. Cultures were incubated for 7 days, after which they were fixed with formaldehyde and stained with Giemsa. The number of colonies was counted to determine the survival fraction.

Determination of the mutant frequency. To determine bystander mutation, 2×10^5 cells were plated evenly on 12 single-well chamber slides, resulting in ~16,666 cells per slide and incubated for 2 hours to allow for cell attachment. After incubation, 0.3% CD59 antiserum and 1.5% (v/v) rabbit serum complement (Covance, Denver, PA) were added as described (15). The slides were incubated for 7 days to allow for mutant colony formation. A_L cells become sensitive to the CD59 antibody in the presence of complement leading to lyses. However, A_L cells that are mutated at the CD59 marker become resistant and proliferate to form colonies.

Quantification of bystander mutants. Because the separation of A_L and CHO cells by magnetic cell separation may not be entirely efficient, it was necessary to differentiate between the two types of colonies by implementing immunofluorescent staining of human chromosome 11 present in A_L cells. The chamber slides with colonies were fixed, probed for human chromosome 11 by fluorescent *in situ* hybridization (FISH) using a peptide nucleic acid (Applied Biosystems, Farmingham, MA) targeted toward the centromeres as described (16). However, mutants that may have lost the entire centromere would not be detected. Positive A_L colonies were scored with the use of a confocal microscope. The mutant fraction at each dose was calculated as the number of surviving mutant colonies divided by the product of the total number of cells plated and the plating efficiency due to the presence of complement alone.

PCR analysis of mutant spectrum. Mutants were independently generated in 30 × 10-mm dishes and two mutants were isolated from each dish. The colonies were expanded in T-25 flasks, had their DNA extracted, and PCR analysis done as described (17, 18). Five marker genes on human chromosome 11 (Wilms' tumor, parathyroid hormone, catalase, RAS, and apolipoprotein A-1) were subjected to PCR analysis based on their mapping positions relative to the *CD59* gene. Amplifications were done for 30 cycles by using a DNA thermal cycler model 480 (Perkin-Elmer/Cetus) in a 20 μL reaction mixture containing 0.2 μg DNA sample in 1× Stoffel fragment buffer, the four deoxynucleotide triphosphates, 3 mmol/L $MgCl_2$, 0.2 mmol/L of each primer, and 2 units Stoffel fragment enzyme. The PCR reaction cycle was composed of denaturation at 94°C for 1 minute, annealing at 55°C for 1 minute, and extension at 72°C for 1 minute. The PCR products were electrophoresed on 3% agarose gels and stained with ethidium bromide.

Statistical analysis. Data for cytotoxicity and mutation were calculated as means and SDs of such means. Statistical significance of survival fractions and mutant fractions was determined by the Student's t test. $P \leq 0.05$ between groups was considered to be statistically significant.

Results

Efficiency of the magnetic separation of A_L and Chinese hamster ovary cells. This study is primarily focused on the bystander response among neighboring A_L cells adjacent to directly labeled CHO cells. To evaluate biological responses only in the bystander A_L cells, the two cell types were segregated by a magnetic cell separation technique. The competence of such a technique was confirmed by using flow cytometric analysis of the two cell populations. When 20% of CHO cells were mixed with 80% of A_L cells containing the human chromosome 11 encoded CD59 surface antigens, the latter was purified by using magnetic beads coated with FITC-conjugated secondary antibodies that bind to the A_L cells. Figure 1 depicts the results of the A_L fraction after magnetic bead purification (Fig. 1*C*) and subjected to flow cytometric analysis. The purity of the A_L fraction was determined to be 99.24%. The controls were unstained CHO (Fig. 1*A*) and unstained A_L (Fig. 1*B*) cells.

Activity of ^3H in A_L and Chinese hamster ovary cell populations after magnetic separation. It is critical that [^{3}H]dTTP from directly labeled CHO cells does not enter the bystander A_L cells within the cluster. The direct labeling of A_L cells can result in an exacerbation of the bystander cytotoxicity and mutagenesis. To establish that there was no incorporation of radioactivity into bystander A_L cells, the ^3H activity of the cell populations was measured after magnetic separation. The directly labeled CHO cell fraction had radioactivity of 2,250,850 cpm, whereas that of the bystander A_L population was only 6,775 cpm or 0.3% that of the CHO cells.

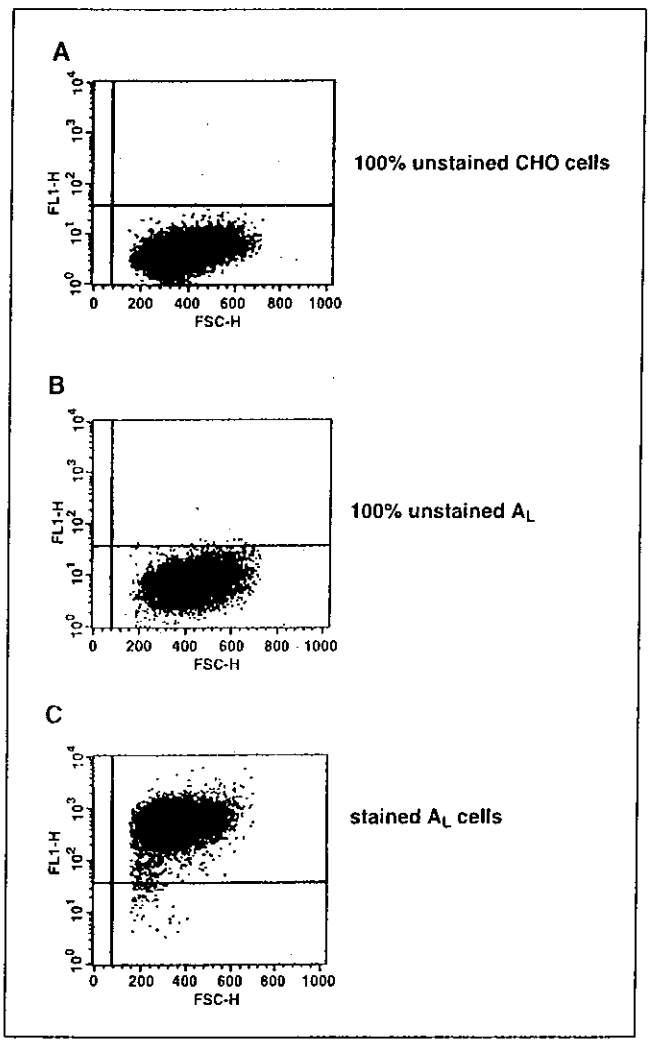

Figure 1. Flow cytometric analysis of clusters of A_L/CHO cells after magnetic separation. Each cluster is composed of 20% CHO and 80% A_L cells. *A* and *B*, 100% control unstained CHO and A_L cells, respectively. *C*, purity of the A_L cell fraction is 99.24% after separation from CHO cells.

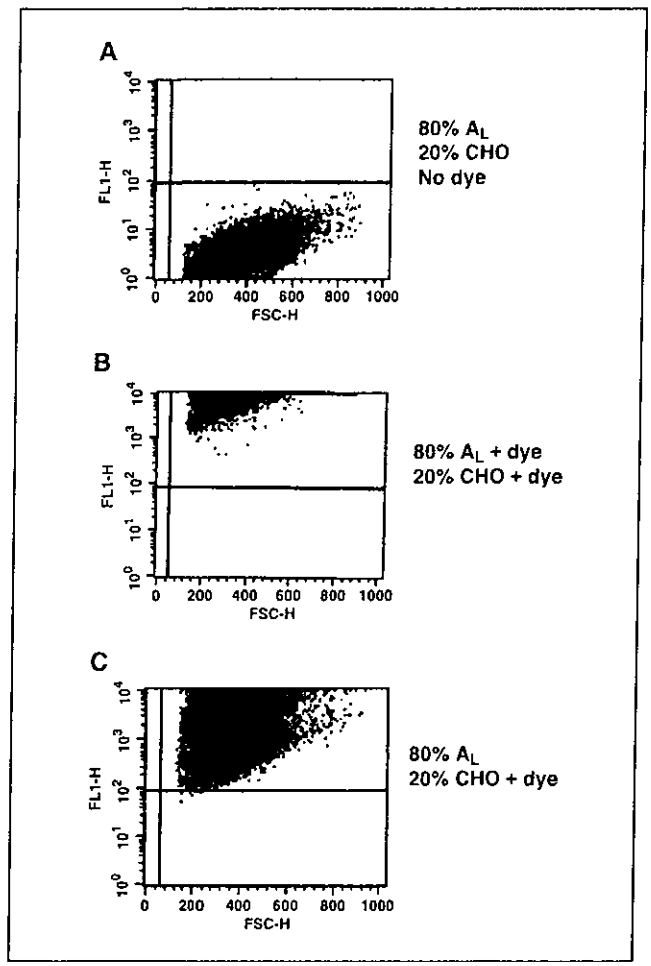

Figure 2. Flow cytometric analysis to show the formation of functional gap junctions between A_L and CHO cells in cluster. *A*, 80% nondyed A_L and 20% nondyed CHO cells. *B*, 100% dyed A_L and CHO cells. *C*, 20% dyed CHO cells cocultured with 80% nondyed A_L cells.

Gap junctional intercellular communication between Chinese hamster ovary and A_L cells in cluster. The transfer of the dye Calcein M was used to establish the formation of gap junctions between cells of the mixed population. Once taken up by CHO cells, the dye can only traverse to neighboring A_L cells through such junctions (5). As indicated by Fig. 2, when only the CHO cell population was exposed to Calcein M with subsequent coculturing with A_L cells in a cluster, 100% of the cell population, including the A_L cells, acquired the dye as shown in Fig. 2*C*. Figure 2*A* shows control, nondyed CHO, and nondyed A_L cells, and Fig. 2*B* shows 100% dyed cells.

Cytotoxicity of Chinese hamster ovary and bystander A_L cells in cluster. Figure 3 shows the dose-response relationship for clonogenic survival of previously directly labeled CHO cells and

nonlabeled neighboring bystander A_L cells after 24 hours of coculture in a cluster where the ratio of CHO-to-A_L cells was 1:5. The clusters consisted of 4×10^6 cells of which 8×10^5 were CHO cells and 3.2×10^6 were A_L cells. At the highest dose of 100 μCi [^{3}H]dTTP, survival fractions for CHO and A_L cells were 0.37 ± 0.04 and 0.56 ± 0.05, respectively, corresponding to a significant difference ($P < 0.05$) in survival compared with their respective controls. It was obvious from these data that the nonirradiated cells showed a strong bystander effect in the mixed culture.

Mutagenicity of bystander A_L cells in cluster with Chinese hamster ovary cells exposed previously to 100 μCi [^{3}H]dTTP. The bystander A_L cells were cultured for 7 days to allow for clonal expansion and expression, after which they were analyzed for mutagenesis. As shown in Fig. 4*A*, when 80% of A_L cells were mixed with 20% of nonlabeled CHO cells, the background CD59$^-$ mutants were $\sim 20 \pm 15$ mutants per 10^5 survivors. In contrast, the CD59$^-$ mutant fraction increased to 270 ± 53 mutants per 10^5 survivors when A_L cells were mixed with 20% of labeled CHO cells, an increase of 14-fold ($P < 0.05$) above background.

Mutant spectrum analysis. Multiplex PCR was used to determine the types of mutations associated with the CD59$^-$ phenotype in the bystander A_L cells. Individual clones were isolated and analyzed for five human chromosome 11 markers located on either side of the *CD59* gene. A total of 190 mutants were analyzed, including 41 of spontaneous origin. As shown in Fig. 4*B*, 59% of the spontaneous CD59$^-$ mutants retained all of the markers. By contrast, 80% of the bystander CD59$^-$ mutants serving as bystanders to CHO cells directly labeled with 100 μCi [^{3}H]dTTP had lost at least one additional marker. This included 44% that lost a minimum of three additional markers. These data indicated that deletion mutations occur at a higher frequency in bystander CD59$^-$ mutants from clusters with 20% of ^{3}H-labeled CHO cells than in clusters with nonlabeled CHO cells.

Role of reactive oxygen species in bystander mutagenesis. To determine whether reactive oxygen species contribute to bystander mutagenesis resulting from low LET exposure, the radical scavenger DMSO was incorporated into the clusters. As shown in Fig. 5, 0.2% DMSO was not cytotoxic and nonmutagenic to the A_L cells because the survival fraction and the mutant fraction were almost identical to that of control. When DMSO was incorporated into the cells in the cluster and maintained throughout the incubation period, the bystander mutation frequency was reduced from 118 ± 30 per 10^5 survivors to 63 ± 12 per 10^5 survivors, corresponding to a 50% reduction. These data indicated that free radicals, mainly hydroxyl radicals, may participate in the pathway leading to bystander mutagenesis.

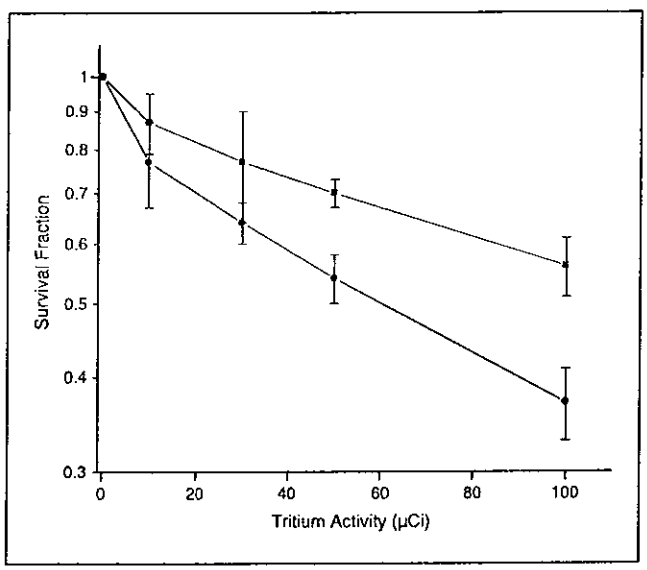

Figure 3. Survival of bystander A_L cells (■) in cluster with CHO cells (●) labeled with graded doses of [^{3}H]dTTP. *Points*, mean of three to four experiments; *bars*, SD.

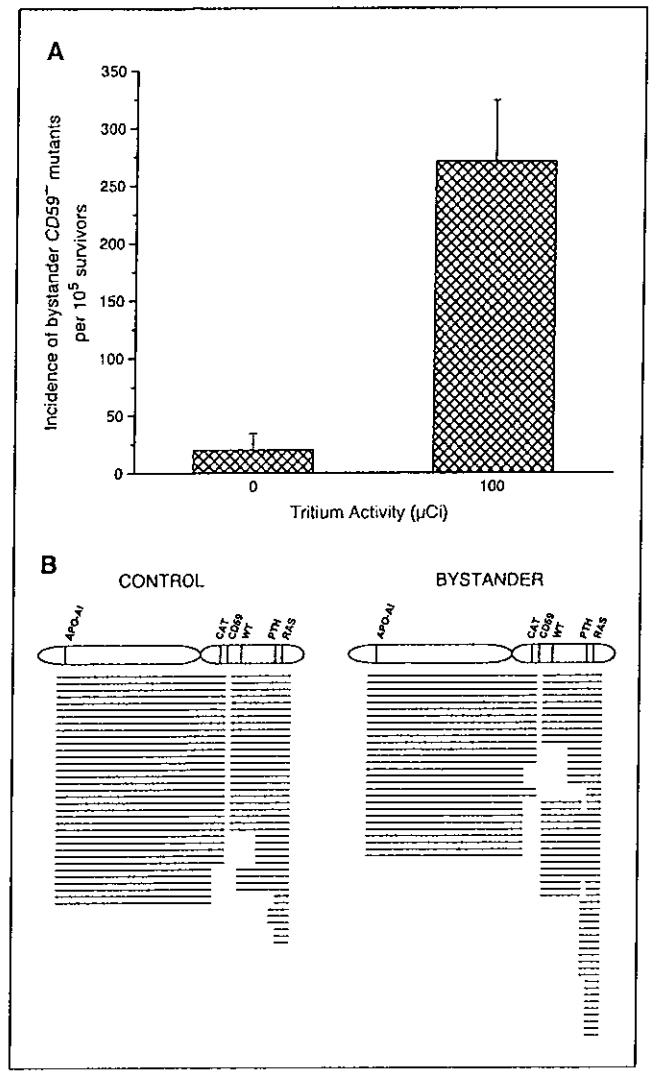

Figure 4. *A*, incidence of bystander CD59$^-$ mutants among A_L cells clustered with CHO cells that were either labeled with 100 μCi [^{3}H]dTTP or no labeling. *Columns*, mean of four experiments; *bars*, SD. *B*, mutant spectrum of bystander CD59$^-$ mutants among A_L cells clustered with CHO cells that were either labeled with 100 μCi [^{3}H]dTTP or no labeling.

Role of cell-to-cell communication in bystander mutagenesis. Previous studies from this laboratory and others have shown that Lindane can inhibit cell-to-cell communication (19–21). To evaluate the contribution of cell-to-cell communication between directly labeled CHO cells and neighboring nonlabeled bystander A_L cells, experiments were conducted by using Lindane, an inhibitor of gap junctional intercellular communication, within the cluster. Figure 6 shows that Lindane was able to significantly decrease the mutant fraction from 174 ± 26 per 10^5 survivors to

84 ± 17 per 10^5 survivors, representing a 52% reduction in mutant fraction. In addition, using connexin 43–deficient A_L cells resulted in a reduction of the bystander mutant fraction from 291 ± 17 per 10^5 survivors to 17 ± 4 per 10^5 survivors, representing a complete attenuation (Fig. 7).

Discussion

This study used a three-dimensional multicellular cluster, with two cell types, CHO and A_L, which were separated after incubation and analyzed as two independent cell populations, the directly labeled versus bystander populations, respectively. There were five times more A_L cells than CHO cells in the cluster. The CHO cells were directly labeled with [^{3}H]dTTP that was incorporated into their DNA, and A_L cells served as bystanders. The mean energy of β-particles emitted from ^{3}H is only 5.7 keV. This is equivalent to a range of only 1 μm in water (22). Because the diameter of a CHO cell nucleus is roughly 7 to 8 μm, nearly all the cells will be self-irradiated with little probability that the β-particles will be able to exit the CHO nucleus and hit neighboring, bystander A_L cells in the cluster. To ensure that A_L bystanders were not directly labeled by [^{3}H]dTTP, two separate approaches were undertaken. First, labeled CHO cells were washed thoroughly to remove any trace of extracellular radioactivity before mixing with the A_L cells. After the final centrifugation to establish the cell clusters, the supernatants were recovered and found to have minimum radioactivity. Second, after the magnetic separation, the radioactivity of the enriched A_L cell population was determined to be 0.3% of the directly labeled CHO cells. This level of activity can be attributed to the few directly labeled CHO cells that may be present in the A_L cell fraction because the efficiency of separation was found to be only 99.24%. Another concern is the possibility of tritium release from CHO cells undergoing apoptosis. However, CHO cell DNA fragments from the apoptotic process are too large to cross the cell membrane and be taken up by A_L cells. Therefore, it implies that any detrimental effects detected among bystander A_L cells will most certainly result from signals originating in directly labeled CHO cells. Bystander A_L cells can respond to mediators from CHO cells because they are

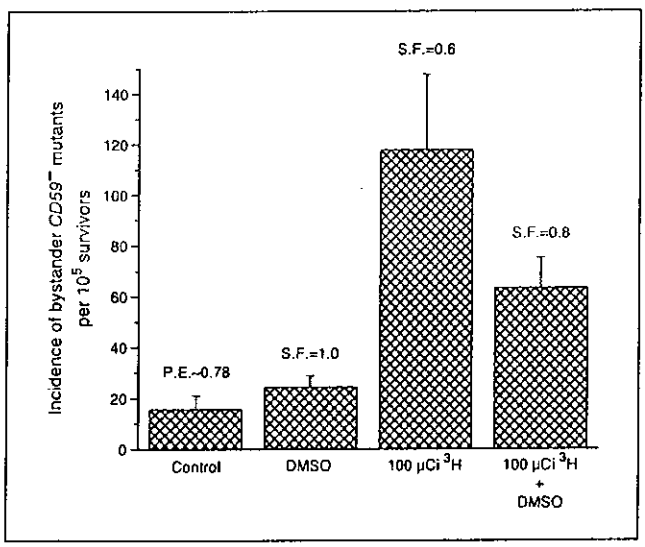

Figure 5. Effect of DMSO (0.2%) on the incidence of bystander CD59⁻ mutants among A_L cells in cluster with CHO cells exposed previously to 100 μCi [^{3}H]dTTP. *Columns*, mean of three experiments; *bars*, SD.

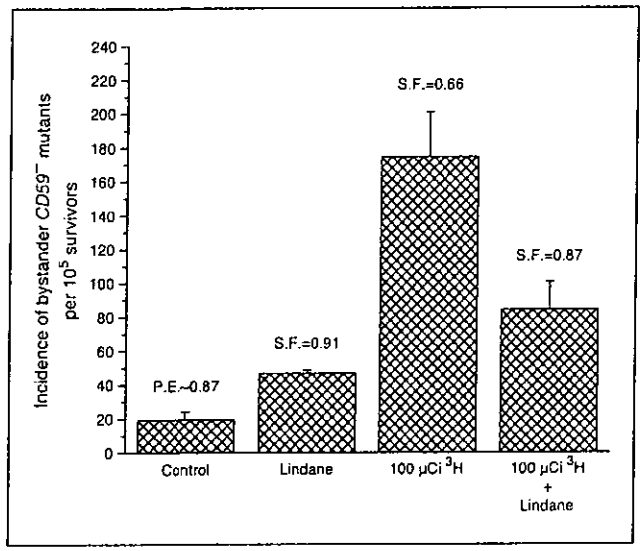

Figure 6. Effect of Lindane (40 μmol/L) on the incidence of bystander CD59⁻ mutants among A_L cells in cluster with CHO cells exposed previously to 100 μCi [^{3}H]dTTP. *Columns*, mean of three experiments; *bars*, SD.

CHO cells in lineage, although A_L cells contain a single copy of human chromosome 11.

The direct labeling of a target population of cells and subsequent incorporation of nonlabeled cells is another approach toward investigating the low LET radiation–induced bystander phenomenon. The other commonly used techniques involved medium-mediated experiments (2, 23) and targeted approaches, such as microbeams (8, 9), where the radiation insult is temporary and the irradiated and nonirradiated cells are analyzed together. In the present study, the incorporation of ^{3}H into the DNA of directly labeled CHO cells will emit β-particles that deposit their energy therein throughout the 24-hour incubation period. For the other techniques, the initial insult lasts only a few seconds; thus, any bystander response produced by nonirradiated cells depends mainly on mediators released into the environment and/or a traversal of signals through gap junctions between targeted and nontargeted cells. For diagnostic or therapeutic purposes, exposure to low LET radiation is relatively short term; thus, any bystander response will propagate from the initial interaction with the impending radiation as can be shown *in vitro* by medium-mediated bystander experiments. However, in terms of occupational or environmental exposure, the duration is usually long term and becomes more significant if the radionuclide enters the biological system. The present work will, therefore, provide significant insight into occupational or environmental exposure, such as that associated with Department of Energy cleanup operations and space travel.

Previous bystander studies with β-particles have shown cell lethality as the major end point of the bystander effect (3–5). The present study is the first to report that mutagenesis, as well as cell lethality, occurs in neighboring bystander A_L cells clustered with directly labeled CHO cells. Because the observed incidence of mutation was a measurement of changes on the single copy of human chromosome 11 present in the human-hamster hybrid A_L cells, it was probable that mutational changes were also imparted to the hamster genome in the hybrid A_L cells and may have contributed to cytotoxicity. The 0.56 survival fraction observed for bystander A_L cells was equated with a 14-fold increase in bystander

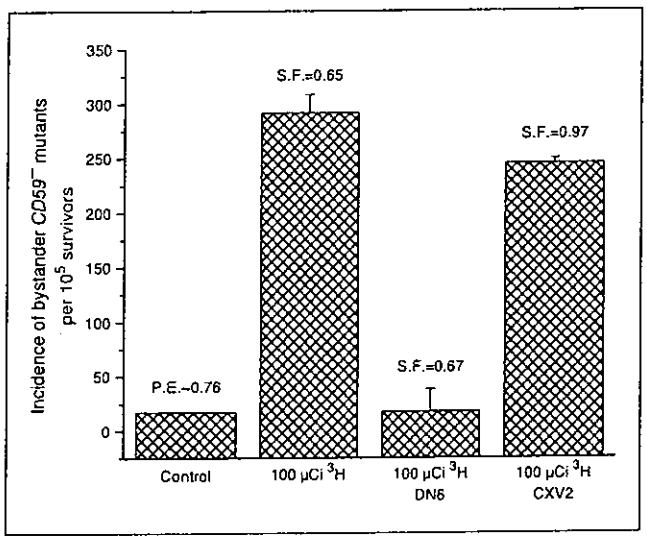

Figure 7. Incidence of bystander CD59⁻ mutants among connexin 43–deficient A_L cells (*DN6*) and empty vector-transfected A_L cells (*CXV2*) clustered with CHO cells that were either labeled with 100 μCi [^{3}H]dTTP or no labeling. *Columns*, mean of three experiments; *bars*, SD.

mutation incidence. A 10-fold transformation yield was observed previously in neighboring cells in proximity to cells also exposed to β-particles (6). The background mutation incidence of 20 ± 15 mutants per 10^5 survivors was relatively lower than reported previously (20). This can be attributed to the magnetic separation technique used to partition the clusters into the A_L and CHO fractions. This procedure uses affinity binding of an antibody toward the CD59 cell surface antigen on A_L cells. Only CD59$^+$ A_L cells will be immobilized on the separation column and become available for the CD59 antibody-complement mutation assay. In addition, CHO cells present in the bystander A_L fraction after magnetic separation can proliferate and be mistaken for mutant colonies. To score only A_L mutant colonies, the centromeres of the human chromosome 11 in the cells were probed by a peptide nucleic acid using FISH. The sequence of the probe is complementary to that of centromeres found in human chromosomes only. This implies there will be no cross-reactivity with hamster chromosomes; thus, only A_L mutant colonies will be stained and scored. However, mutants that have lost the entire centromeric region will not be scored leading to an underestimation of the mutant fraction. CD59-deficient cells that are lacking the centromere can arise following exposure to sparsely ionizing radiation (24); thus, it is likely that the procedures used for mutant selection in the present study underestimate the true CD59 mutant fraction. This limitation may also induce bias toward the observed mutant spectra for both control and treated cultures depending on the proportion of mutants that have lost the centromeric region. Nevertheless, the underestimated mutant yield will not change the observed bystander mutagenic yield or the conclusions drawn. Furthermore, a partial loss of the centromere will not affect the efficiency of detection as the probe does not require the complete sequence of bases.

The significant increase in cell lethality and mutation incidence indicated a potent bystander signal or a significant amplification of the bystander response especially because there were five times more bystander A_L. The three-dimensional cluster conformation provides more effective interaction of mediators because there is more contact between the cell types compared with a two-dimensional model. The cluster model also prevents any considerable dilution of secreted mediators. The mutation spectra obtained for the bystander A_L cells was able to complement the observed mutation incidence. A significant number of multilocus deletions were observed in the majority of clones. Similar spectra were generated from direct exposure of A_L cells to X-rays and A_L cells to nitrogen and proton ions that target the entire population of cells (10, 24). The overlap of mutation spectra implies that similar mediators may be responsible for mutagenesis arising from the bystander response or direct exposure to low LET radiation. It must be noted that the reduction in metabolic activity as a consequence of incubation at 11°C may influence the magnitude of the bystander signals and counter response.

The β-particles emitted from ^{3}H incorporated into the DNA of targeted CHO cells deposit energy that may ionize water molecules in the vicinity leading to the initiation of lipid peroxidation, a probable initial event. The data obtained from the utilization of DMSO suggest that reactive oxygen species, mainly hydroxyl radicals, a potent initiator of lipid peroxidation, may be involved in the early stages of the cascade sequence. Bishayee et al. (5) provided evidence to support this finding with low LET radiation by using ^{3}H in a multicellular cluster with cell lethality as the end point. However, with high LET α-particles, DMSO did not inhibit the bystander mutagenic response in nonirradiated neighboring cells (20). These observations suggest that the type of radiation may influence the mediators and pathways involved in the bystander response.

The cluster of CHO and A_L cells allows for intimate contact between the different types of cells. The migration of the fluorescent dye Calcein M from dyed CHO cells to nondyed A_L cells justified the formation of functional gap junctions allowing for intercellular communication. The present finding that Lindane provides protection against the low LET radiation–induced bystander response is consistent with these observations. To further confirm the role of intercellular communication, A_L cells, dominant negative for connexin 43 that will impair gap junction formation, were used to evaluate bystander mutagenesis. In such cells, there was complete attenuation of the bystander mutagenic response.

The actual mediator or signal that influences neighboring bystander A_L cells to elicit responses remains to be identified. The size of molecules that can traverse gap junctions is usually <1,500 Da (25) and can include a myriad of ions and small molecules. The reactive oxygen species that may be generated by the ionization of water are short-lived and can only migrate distances significantly smaller than the diameter of cells; thus, oxyradicals are unlikely to be directly responsible for the bystander effect. It is plausible that the generation of reactive oxygen species is among the preliminary events that occur in CHO cells incorporating ^{3}H. This can subsequently lead to the synthesis and/or secretion of molecules, small peptide mediators, or sequestered ions into the intercellular space or through gap junctions. Secretion of such might lead to interaction with the membrane or intracellular components of neighboring bystander A_L cells possibly leading to the initiation of a second messenger system. Because the cells are in clusters for 24 hours with continuous insult, this may result in the synthesis of secondary mediators that are not normally present in any significant concentrations. From medium-mediated and microbeam experiments where the irradiation time is <1 minute, it suggests that the

initial reaction to the stress is enough to propel the targeted cells to produce bystander mediators.

The present study provides evidence that low LET radiation from directly labeled cells can illicit a mutagenic response in neighboring bystander cells and suggests that a signaling pathway involving reactive oxygen species and/or the secretion of mediator molecules may contribute to the observed bystander effect. Because free radicals are unlikely to traverse cells, it is possible that secreted mediators can induce reactive oxygen species formation in bystander A_L cells that can contribute to cytotoxicity and mutagenesis. The numerous multilocus deletions observed in the mutant colonies suggest that such oxyradicals may be directly involved in the mutation event. The possible utilization of gap junctions for the transmission and propagation of the bystander signal to adjacent cells implies that it requires a relatively small number of target cells to elicit a major response. The bystander cytotoxicity and mutagenesis findings of this study are consistent with those from high LET radiation studies with α-particles. Therefore, it implies that risk assessment for low LET radiation exposure may require similar management guidelines as those established for high LET radiation.

Acknowledgments

Received 8/10/2004; revised 7/25/2005; accepted 8/12/2005.

Grant support: Department of Energy grant DE-FG02-03ER63441 from the Low Dose Program and NIH grants CA 49062 and ES 11804.

The costs of publication of this article were defrayed in part by the payment of page charges. This article must therefore be hereby marked *advertisement* in accordance with 18 U.S.C. Section 1734 solely to indicate this fact.

We thank Drs. Vladimir Ivanov and Adayabalam Balajee for providing invaluable suggestions.

References

1. Hall EJ, Hei TK. Genomic instability and bystander effects induced by high-LET radiation. Oncogene 2003; 22:7034–42.
2. Mothersill C., Seymour CB. Medium from irradiated human epithelial cells but not human fibroblasts reduces the clonogenic survival of unirradiated cells. Int J Radiat Biol 1997;71:421–7.
3. Bishayee A, Rao DV, Howell RW. Evidence for pronounced bystander effects caused by nonuniform distributions of radioactivity using a novel three-dimensional tissue culture model. Radiat Res 1999;152: 88–97.
4. Bishayee A, Rao DV, Bouchet LG, Bolch WE, Howell RW. Protection by DMSO against cell death caused by intracellularly localized iodine-125, iodine-131 and polonium-210. Radiat Res 2000;153:416–27.
5. Bishayee A, Hill HZ, Stein D, Rao DV, Howell RW. Free radical-initiated and gap junction-mediated bystander effect due to nonuniform distribution of incorporated radioactivity in a three-dimensional tissue culture model. Radiat Res 2001;155:335–44.
6. Sigg M, Crompton NEA, Burhart W. Enhanced neoplastic transformation in an inhomogeneous radiation field: an effect of the presence of heavily damaged cells. Radiat Res 1997;148:543–7.
7. Schettino G, Folkard M, Prise KM, Voynovic B, Held KD, Michael BD. Low-dose studies of bystander cell killing with targeted soft X rays. Radiat Res 2003;160: 505–11.
8. Schettino G, Folkard M, Prise KM, Voynovic B, Bowey AG, Michael BD. Low-dose hypersensitivity in Chinese hamster V79 cells targeted with counted protons using a charged-particle microbeam. Radiat Res 2001;156:525–34.
9. Prise KM, Folkard M, Malcolmson AM, et al. Single ion actions: the induction of micronuclei in V79 cells exposed to individual protons. Adv Space Res 2000;25: 2095–101.
10. Wedemeyer N, Greve B, Uthe D, et al. Frequency of CD59 mutations induced in human-hamster hybrid A_L cells by low-dose X-irradiation. Mutat Res 2001;473: 73–84.
11. Mognato M, Bortoletto E, Ferraro P, et al. Genetic damage induced by *in vitro* irradiation of human G_0 lymphocytes with low-energy protons (28 keV/μm): HPRT mutations and chromosomal aberrations. Radiat Res 2003;160:52–60.
12. Xue LY, Butler NJ, Makrigiorgos GM, Adelstein SJ, Kassis AI. Bystander effect produced by radiolabeled tumor cells *in vivo*. Proc Natl Acad Sci U S A 2002;99: 13765–70.
13. Watson GE, Lorimore SA, Macdonald DA, Wright EG. Chromosomal instability in unirradiated cells induced *in vivo* by a bystander effect of ionizing radiation. Cancer Res 2000;60:5608–11.
14. Waldren CA, Jones C, Puck TT. Measurement of mutagenesis in mammalian cells. Proc Natl Acad Sci U S A 1979;76:1358–62.
15. Zu L, Waldren CA, Vannais D, Hei TK. Cellular and molecular analysis of mutagenesis induced by charged particles of defined LET. Radiat Res 1996;145:251–9.
16. Williams B, Stender H, Coull JM. PNA fluorescent *in situ* hybridization for rapid microbiology and cytogenetic analysis. In: Nielsen PE, editor. Peptide nucleic acids: methods and protocols. Totowa (NJ): Humana Press; 2002. p. 181–93.
17. Hei TK, Wu LJ, Liu SX, Vannais D, Waldren CA, Randers-Pehrson G. Mutagenic effects of a single and exact number of α particles in mammalian cells. Proc Natl Acad Sci U S A 1997;94:3765–70.
18. Hei TK, Piao CQ, He ZY, Vannais D, Waldren CA. Chrysotile fiber is a potent mutagen in mammalian cells. Cancer Res 1992;52:6305–9.
19. Azzam EI, de Toledo SM, Gooding T, Little JB. Intercellular communication is involved in the bystander regulation of gene expression in human cells exposed to very low fluences of α particles. Radiat Res 1998;150: 497–504.
20. Zhou H, Randers-Pehrson G, Waldren CA, Vannais D, Hall EJ, Hei TK. Induction of a bystander mutagenic effect of α particles in mammalian cells. Proc Natl Acad Sci U S A 2000;97:2099–104.
21. Shao C, Furusawa Y, Aoki M, Ando K. Role of gap junctional intercellular communication in radiation-induced bystander effect in human fibroblasts. Radiat Res 2003;160:318–23.
22. ICRU Publication 37. Stopping powers for electrons and positrons. Bethesda (MD): International Commission on Radiation Units and Measurements; 1984.
23. Shao C, Aoki M, Furusawa Y. Medium-mediated bystander effects on HSG cells co-cultivated with cells irradiated by X-rays or a 290 MeV/μ carbon beam. J Radiat Res 2001;42:305–16.
24. Kraemer SM, Kronenberg A, Ueno A, Waldren CA. Measuring the spectrum of mutation induced by the human-hamster hybrid cell line A_LC. Radiat Res 2000; 153:743–51.
25. Prise KM, Folkard M, Michael BD. Bystander responses induced by low LET radiation. Oncogene 2003;22:7043–9.